

**Rock-Fabric Petrophysical Analysis of Core and Wireline-Log Data
Haradh 101 and Haradh 106
Ghawar Field, Saudi Arabia**

F. Jerry Lucia and Michael A. Rahnis

Final Report

prepared to fulfill requirements of ASC
Contract No. 710315/00 between Aramco Services
Company and The University of Texas at Austin

Bureau of Economic Geology
Noel Tyler, Director
The University of Texas at Austin
Austin, Texas 78713-8924

February 1998

*Received
3/23/98*

LR

3/27/98

*Ed,
Please verify
that you have a
copy of this
report. Thanks.*

Lynnda

**Rock-Fabric Petrophysical Analysis of Core and Wireline-Log Data
Haradh 101 and Haradh 106
Ghawar Field, Saudi Arabia**

F. Jerry Lucia and Michael A. Rahnis

Final Report

prepared to fulfill requirements of ASC
Contract No. 710315/00 between Aramco Services
Company and The University of Texas at Austin

Bureau of Economic Geology
Noel Tyler, Director
The University of Texas at Austin
Austin, Texas 78713-8924

February 1998

CONTENTS

Abstract	1
Introduction.....	2
Statement of Problem	4
Rock-Fabric-Specific Permeability Transforms.....	4
Method.....	4
Sampling Problems, Problems of Scale	7
Limestone (0 to 10-percent dolomite)	9
Grainstone.....	9
Grain-Dominated Packstone	9
Mud-Dominated Fabrics.....	13
Dolomitic Limestones (10- to 80-Percent Dolomite)	18
Dolomitic Grain-Dominated Packstones.....	18
Dolomitic Mud-Dominated Fabrics.....	18
Dolostone	22
Porosity-Permeability Transforms	26
Permeability from Wireline Logs	29
Approach	29
Calculation of Interparticle Porosity.....	30
Determination of Rock-Fabric Petrophysical Class	34
Permeability Calculation from Wireline Logs.....	39
Conclusions	39
References	45
Appendix 1	47

Figures

1. Location map of the Haradh area, Ghawar field, showing structural contours and location of Haradh 101 and 106 wells	3
2. Cross plots of core data from Haradh 101 and 106	5
3. Frequency plot of percent dolomite in samples from Haradh 101 and 106 showing lithology groupings and cross-plot of core porosity and percent dolomite for samples from Haradh 101 and 106	8
4. Porosity–permeability cross plot for grainstone, showing both total and interparticle porosity	10
5. Photomicrographs of grainstone	11
6. Porosity–permeability cross plot for grain-dominated packstone, showing both total and interparticle porosity	12
7. Cross plots of porosity and permeability against mud content for grain-dominated packstones and mud-dominated fabrics	14
8. Photomicrographs illustrating range of fabrics classified as grain-dominated packstone	15
9. Photomicrographs of permeable mud-dominated fabrics	16
10. Porosity–permeability cross plot for mud-dominated fabrics, showing both total and interparticle porosity	17
11. Porosity–permeability cross plot for dolomitic grain-dominated packstone	19
12. Photomicrographs of dolomitic limestones	20
13. Porosity–permeability cross plot for dolomitic mud-dominated fabrics	21
14. Photomicrographs of dolomitic wackestones illustrating the development of intercrystal porosity	23
15. Porosity–permeability cross plot for dolostones	24
16. Photomicrographs of dolostone	25
17. Porosity–permeability cross plot of all representative samples showing rock-fabric petrophysical classes	27
18. Continuum of rock fabrics and associated porosity–permeability transforms	28
19. Acoustic, porosity, separate-vug relations from wells HRD 101 and 106	32
20. Comparison of separate-vug porosity from logs and thin sections in wells HRDH 101 and 106	33
21. Cross plot of porosity and water saturation showing rock-fabric petrophysical classes	35

22.	Comparison of petrophysical classes from logs and thin sections for well HRDH 101	37
23.	Comparison of petrophysical classes from logs and thin sections for well HRDH 106	38
24.	Comparison of core and log-calculated permeability values for well HRDH 101	40
25.	Comparison of core and log-calculated permeability values for well HRDH 106	41
26.	Diagram summarizing rock fabrics found in thin sections of wells HRDH 101 and 106....	42

ABSTRACT

Analysis of thin sections and core data demonstrates that rock fabrics can be grouped into petrophysical fields defined by porosity and permeability. Grainstones and large crystal dolostones fall within the petrophysical class 1 field of Lucia (1995). Permeability increases with increasing dolomite crystal size. The class 1 field is enlarged slightly to include large crystal dolostones with crystal sizes ranging to 300 microns. Grain-dominated and dolomitic mud-dominated fabrics containing more than 25 percent dolomite fall into the petrophysical class 2 field. The dolomitic mud-dominated fabrics plot in the class 2 field because progressive dolomitization increases pore size by increasing porosity in the intercrystal mud and by creating intercrystal pore space. Mud-dominated fabrics having less than 25 percent dolomite are mostly dense but, when permeable, plot in the petrophysical class 3 field. A global relationship between rock-fabric petrophysical class, interparticle porosity, and permeability that does not require fabrics being divided into specific petrophysical classes has been developed and is used in this analysis.

Permeability can be estimated from wireline logs according to the rock-fabric method. Interparticle porosity is estimated by subtracting total porosity from separate-vug porosity, which, in turn, is estimated from transit-time-porosity cross plots. Petrophysical classes can be identified from a cross plot of water saturation and porosity. The wells are far enough above the free-water level that reservoir height is not an important consideration. We identified boundaries between rock-fabric classes and multiple-regression analysis, using equations of the boundary lines, resulted in a relationship between petrophysical class, saturation, and porosity. Permeability is calculated by substituting log-calculated interparticle porosity and log-calculated petrophysical class into the global transform equation. These calculations compare well with core data and retain high and low permeability values.

It is important to retain the rock-fabric petrophysical class term in this calculation because it provides the link between petrophysical properties and geologic processes necessary to display

permeability, porosity, and water saturation in 3-D. Without the tie to stratigraphy, deposition, and diagenesis, log-calculated petrophysical properties cannot be realistically distributed in 3-D space. Identifying rock fabrics from log-calculated petrophysical classes requires additional information because (1) multiple rock fabrics are in each class, and (2) the saturation approach applies only to permeable intervals. Class 1 includes both large crystal dolomite and grainstone. Lithology can be used to distinguish between them. Class 2 includes grain-dominated packstones, dolomitic grain-dominated packstones, and dolomitic mud-dominated fabrics. Although lithology can be used to distinguish grain-dominated packstones, it cannot distinguish between dolomitic grain-dominated packstones and dolomitic mud-dominated fabrics. Class 3 includes mud-dominated fabrics having less than 25 percent dolomite. Because most dense samples are mud-dominated and dolomitic mud-dominated fabrics, low-porosity intervals are assigned to class 3.

The super k interval in well 101 appears to be producing from a touching-vug pore system composed of small caverns and fractures. The extensive amount of large crystalline dolostone around this touching-vug pore system suggests that this system also provided the flow path for dolomitizing fluids. Assuming that dolomitization is late, the pore space of the precursor limestone may have been similar to the present limestone, and the dolostone may have inherited its porosity values from the precursor limestone. The important impact of dolomitization is the increased pore size in the mud-dominated and grain-dominated packstone fabrics.

INTRODUCTION

This report was prepared to fulfill the requirements of ASC Contract No. 710315/00 between Aramco Services Company and The University of Texas at Austin. The goal of this project was to (1) describe thin sections from two wells in the Haradh area of Ghawar field, (2) correlate the rock fabrics having porosity and permeability and (3) develop methods for determining rock fabrics and permeability from wireline logs. The Haradh 101 and 106 wells were selected by Aramco (fig. 1).

Location — Structure Map, Haradh Area

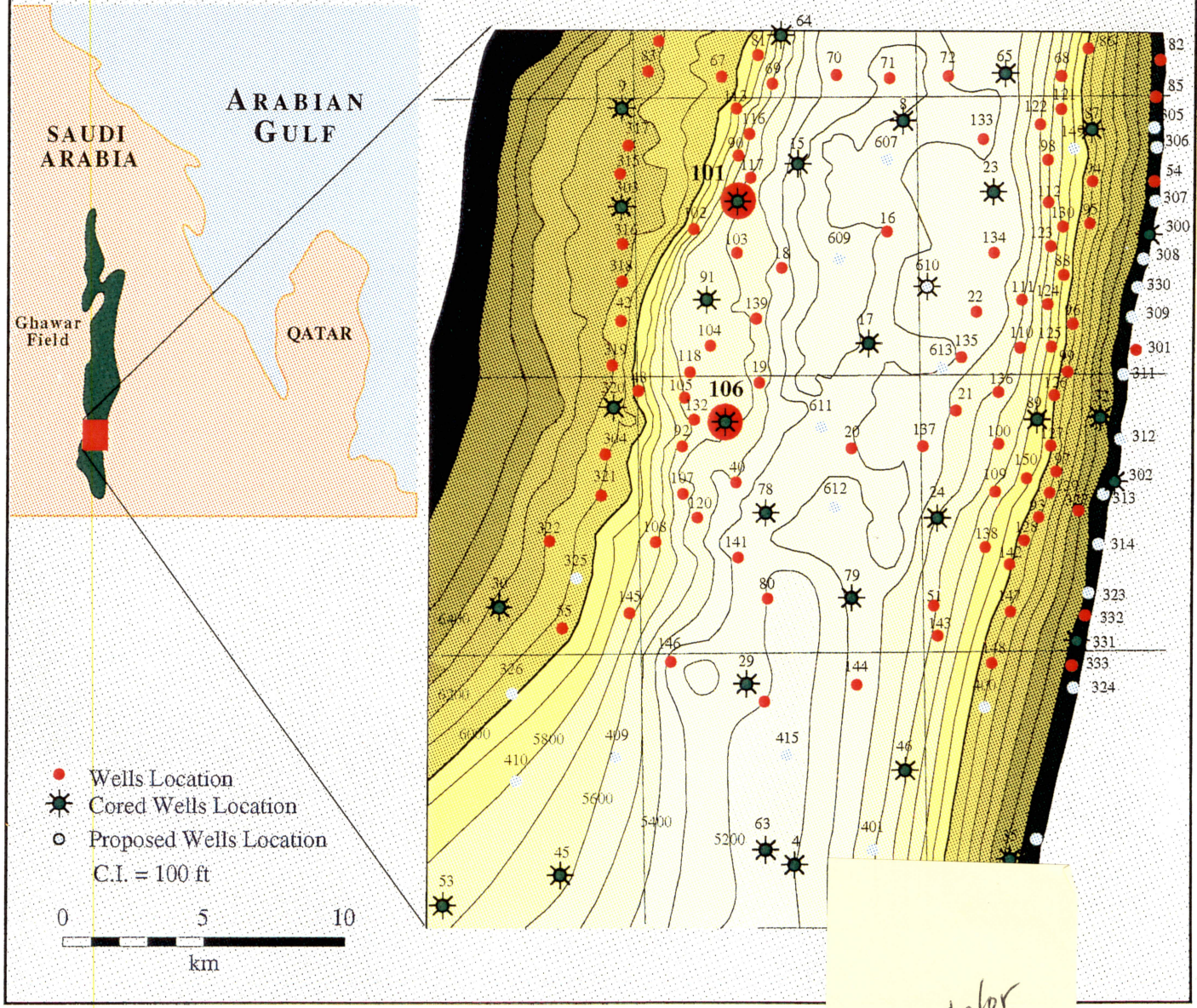


Figure 1. Location map of the Haradh area, Ghawar field, showing wells and location of Haradh 101 and 106 wells (courtesy of Aramco).

Detailed results and interpretations are presented, including analysis of the thin-section descriptions and application of the results to wireline logs.

Statement of Problem

A key to predicting performance accurately using flow simulators is to capture the spatial distribution of high and low permeabilities in the reservoir. Permeability values routinely obtained by core analysis characteristically have an extremely high variance. This is true of the core data from Haradh 101 and 106 (fig. 2A), where permeability values vary from less than 0.01 to 7,000 md. The conventional method of dealing with this extreme variability is to correlate permeability with porosity and construct a porosity-permeability transform. It is generally agreed, however, that single porosity-permeability transforms tend to average out high and low permeabilities.

The method used in this study to maintain high and low permeabilities is referred to as the rock-fabric method. It is based on the fundamental concept that permeability is a function of pore-size distribution, which is directly related to particle size, sorting, interparticle porosity, and touching-vug pore systems (fig. 2B) (Lucia, 1995). Because separate-vug pore space does not contribute greatly to permeability, it must be identified and subtracted from total porosity to obtain interparticle porosity. The approach is to (1) relate core permeability values to rock fabric and interparticle porosity and develop multiple rock-fabric-specific interparticle-porosity, permeability transforms; (2) relate rock fabrics to water-saturation, porosity cross plots from wireline-log analysis; and (3) use rock-fabric-specific transforms to calculate permeability from wireline logs.

ROCK-FABRIC-SPECIFIC PERMEABILITY TRANSFORMS

Method

Rock fabrics are identified from descriptions of samples used to measure petrophysical properties. In this study, 1.25-inch-diameter core plugs were used and the rock-fabric descriptions

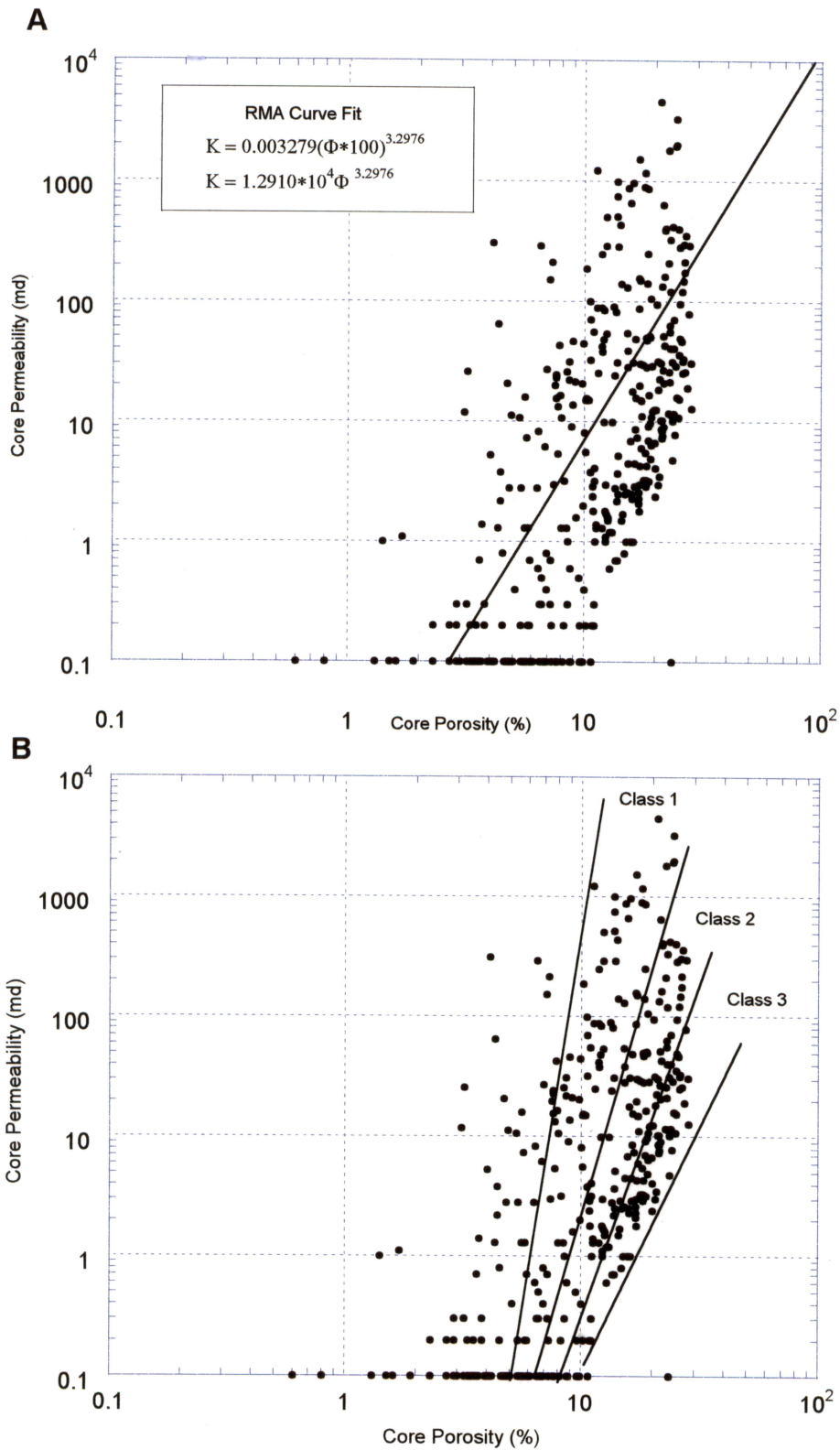


Figure 2. Cross plots of core data from Hardh 101 and 106. (A) Porosity–permeability cross plot showing a Reduced Major Axis fit to the data. (B) Porosity–permeability cross plot showing rock-fabric petrophysical classes that are defined by permeability, interparticle porosity, particle size, and sorting (Lucia, 1995).

are from thin sections of the plug ends. Although sample density is 0.5 ft, in most intervals thin sections were described every foot. A total of 421 thin sections were described and the descriptions are included in appendix 1. We determined percentages of pore types and minerals by 300 point counts per thin section according to mechanical stage. The first step in describing rock fabrics for petrophysical analysis is to divide the pore space into interparticle, separate-vug, and touching-vug pore types. Interparticle pores are visible between grains, dolomite crystals, and within the mud matrix. Separate vugs are found within fossil fragments (forams and *Cladocoropsis*) as grain molds and as intragrain microporosity in grain-dominated fabrics. No touching-vug porosity was noted, although some thin sections contained a few microfractures. Separate-vug porosity ranged from 0 to 7 porosity percent, averaging less than 1 percent. Although intragrain microporosity was found in small quantities in most grain-dominated packstones, it was abundant only in well 101 in the interval between 6,555 and 6,562 ft. Microporosity could not be point counted because of its small size, and estimates were made by counting grains that contained microporosity identified by observing traces of blue dye within the grains. Interparticle porosity was determined by subtracting separate-vug porosity from core-plug porosity. In most cases the difference between total and interparticle porosity was found to be small.

Other measurements that are important to petrophysical characterization are mineralogy, particle size, and sorting. Mineralogy is determined by point counting. Dolomite and calcite account for most of the mineral volume, along with occasional small amounts of anhydrite, chert, and clay. Average grain and crystal size is determined by an ocular micrometer. Sorting is characterized by the Lucia classification; that is, grainstone is well sorted, grain-dominated packstone is moderately sorted, mud-dominated packstones is poorly sorted, and wackestone and mudstone are considered to be well-sorted fine-particle-size fabrics.

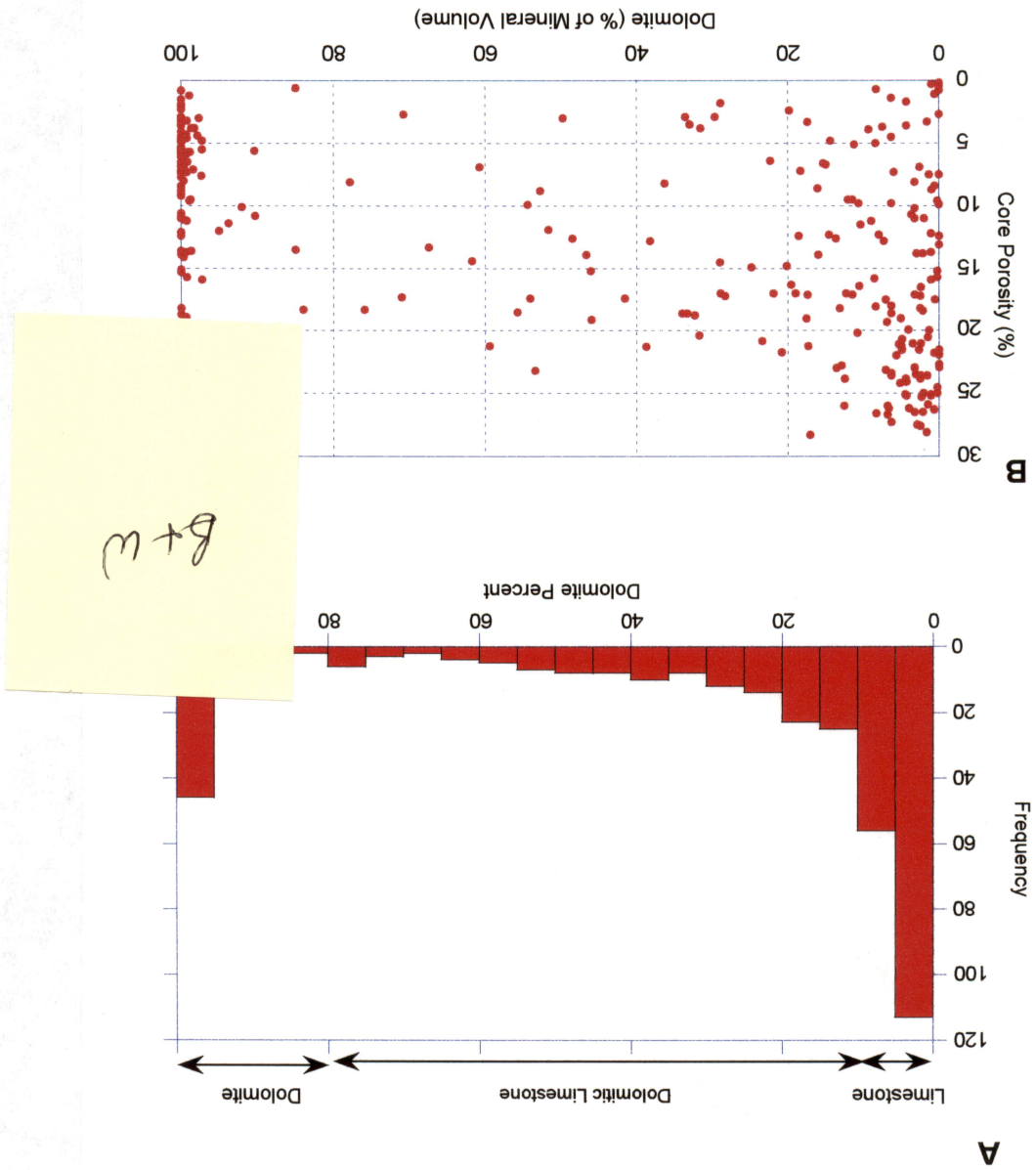
Sampling Problems, Problems of Scale

A concern in this type of study is the degree to which the thin section represents the fabric of the sample that is used to measure the petrophysical property. Although rock-fabric categories are kept broad to cover a range of fabrics, small-scale heterogeneity may cause the plug to be unrepresentative. Examples are (1) patchy distribution of calcite cement, sulfate, dolomite, or micrite; and (2) very large particles, such as fossils. Patchy distribution often results in large differences between thin-section porosity and core-analysis porosity values. It can also be the cause of anomalous permeability values, permeability values that are either too high or too low for the measured porosity, and rock fabric. Two samples were discarded from the data set for this reason, and 38 samples were discarded because they contained large fragments of *Cladocoropsis*. Burrowing fabrics are present in grain-dominated packstones and mud-dominated fabrics, and dolomite is irregularly distributed in the dolomite limestones. These fabrics most likely produce much of the scatter seen within the rock-fabric groups.

A second concern is the difference between reservoir and ambient conditions. Studies have shown that in the Arab D Formation there is little difference between porosity values measured at ambient conditions and those measured under confining pressure (Harari and others, 1995). However, samples having well-developed stylolites commonly have higher than expected permeability values, probably because of the opening of pore space along the stylolites, which results from the reduction of confining pressure when they are brought to the surface. Twenty-eight samples were discarded from the data set because they contained well-developed stylolites.

The principal mineralogical consideration is percent of dolomite. Dolomite content ranges from 0 to 100 percent (fig. 3). For the purposes of this analysis, the samples are divided into limestone (0 to 10-percent dolomite), dolomitic limestone (10- to 80-percent dolomite), and dolomite (80- to 100-percent dolomite) for analysis. The 80-percent limit was chosen because Powers (1962) reported that porosity and permeability increased when between 80- and

Figure 3. (A) Frequency plot of percent dolomite in samples from Haradh 101 and 106 showing lithology groupings. (B) Cross-plot of core porosity and percent dolomite for samples from Haradh 101 and 106. Although there is very little difference in the porosity range, the dolostone has more low porosity values than does the limestone.



100-percent dolomite was present. An increase in porosity with dolomitization has not, however, been observed in this data set (fig. 3).

LIMESTONE (0 TO 10-PERCENT DOLOMITE)

Grainstone

There are only 15 grainstone samples in the sample set, and 4 were discarded on suspicion of their being unrepresentative of the core plug. The 11 remaining samples are porous and permeable and plot in the class 1 field of Lucia (1995) (fig. 4). The grainstones can be divided into two types. The first type is found toward the top of the Arab D. It contains well-sorted, coated grains (200 to 400 mm) having isopachous calcite cement on multicrystal grains and syntaxial-overgrowth cement on single-crystal echinoderm fragments (fig. 5A). Compaction effects include grain interpenetration, grain crushing, and spalling of isopachous cement. As much as 7 percent moldic porosity is found in this grainstone. The second type of grainstone, found in the lower part of the Arab D, is a mixture of 200- to 400-mm and >500-mm peloids (fig. 5B). The grains are probably mudstone intraclasts because they are associated with intervals of mudstone and wackestone fabrics. No cement or separate vugs are apparent in the samples. There is, however, considerable grain penetration, suggesting considerable compaction and associated loss of porosity.

Grain-Dominated Packstone

There are 100 samples of grain-dominated packstones, most of which are porous and permeable. Of these samples, 20 were discarded for having large *Cladocoropsis* grains and 9 for the presence of stylolites. The remaining 71 samples plot within the class 2 field (fig. 6A). The stylolitic samples and a few of the *Cladocoropsis* samples plot to the left of the class 2 field (fig. 6B). The grain-dominated packstones show a wide variety of fabrics because of variations in the mud content related to burrowing of mud into grain-dominated fabrics and grains into mud-

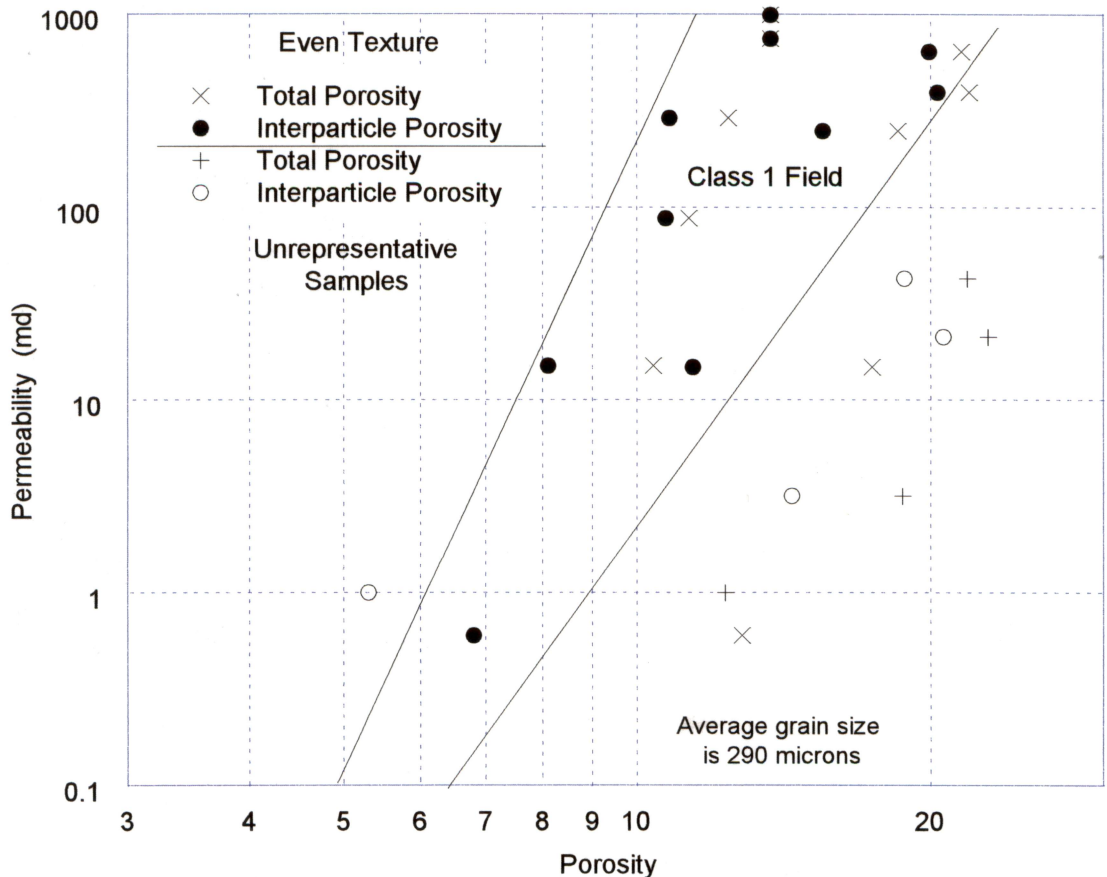
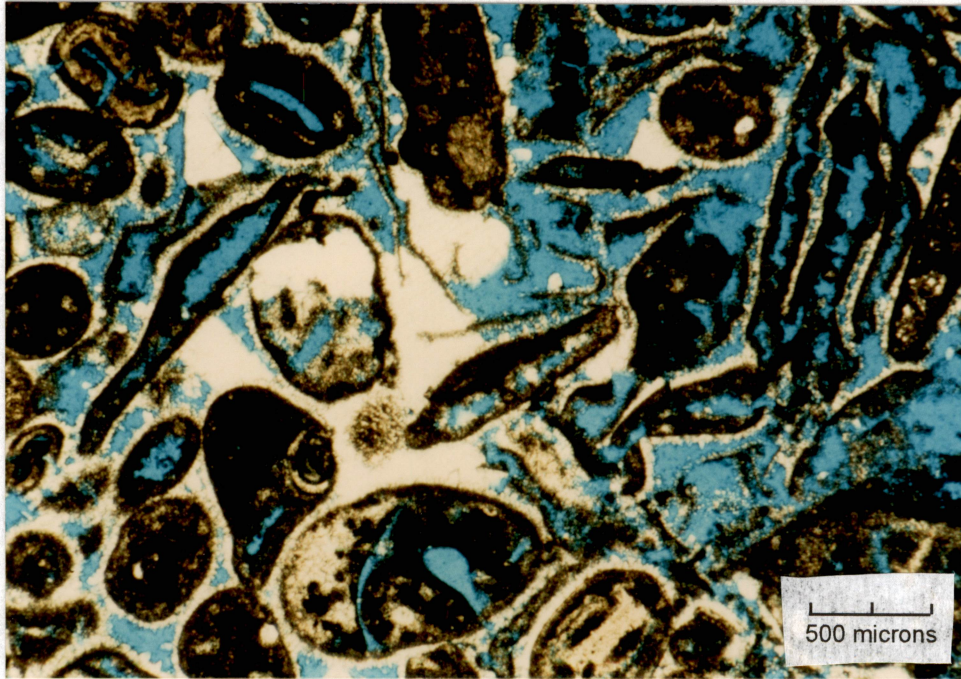


Figure 4. Porosity-permeability cross plot for grainstone, showing both total and interparticle porosity. The difference is separate-vug porosity determined by point counting thin sections. Several samples have 6-percent separate vugs and would plot in the class 2 field using total porosity. Four samples were discarded because the fabrics appear to be unrepresentative of the petrophysical values.

A



B

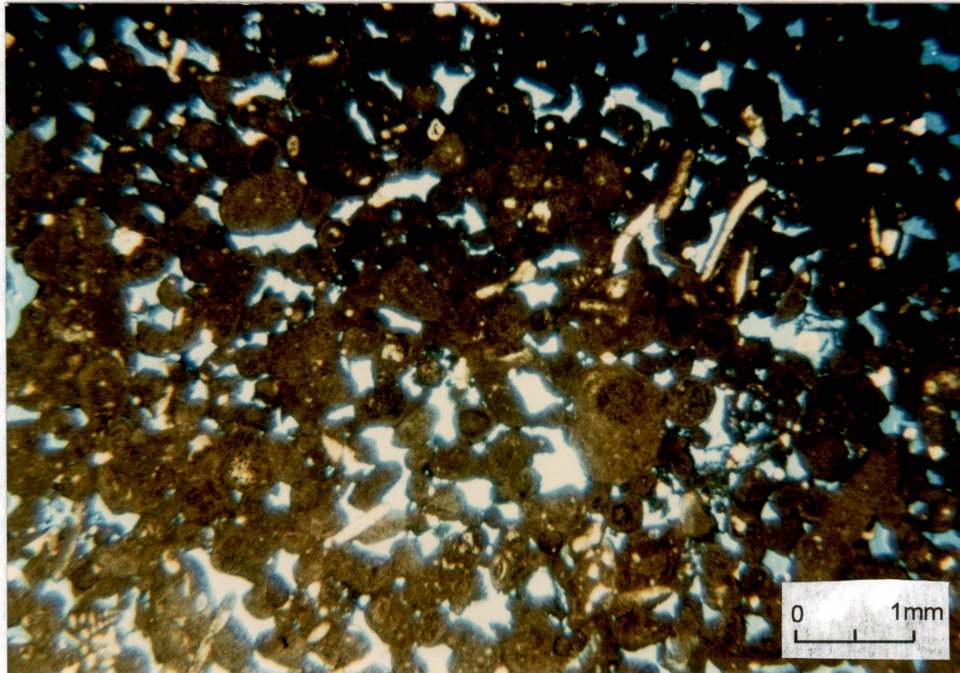


Figure 5. Photomicrographs of grainstone. (A) Fossil grainstone from PSS 8 zone. ($\phi_{ip} = 11.4\%$, $Sv_{ug} = 6\%$, $k = 14.9$ md). (B) Peloid grainstone from lower interval ($\phi_{ip} = 13.7\%$, $k = 997.3$ md).

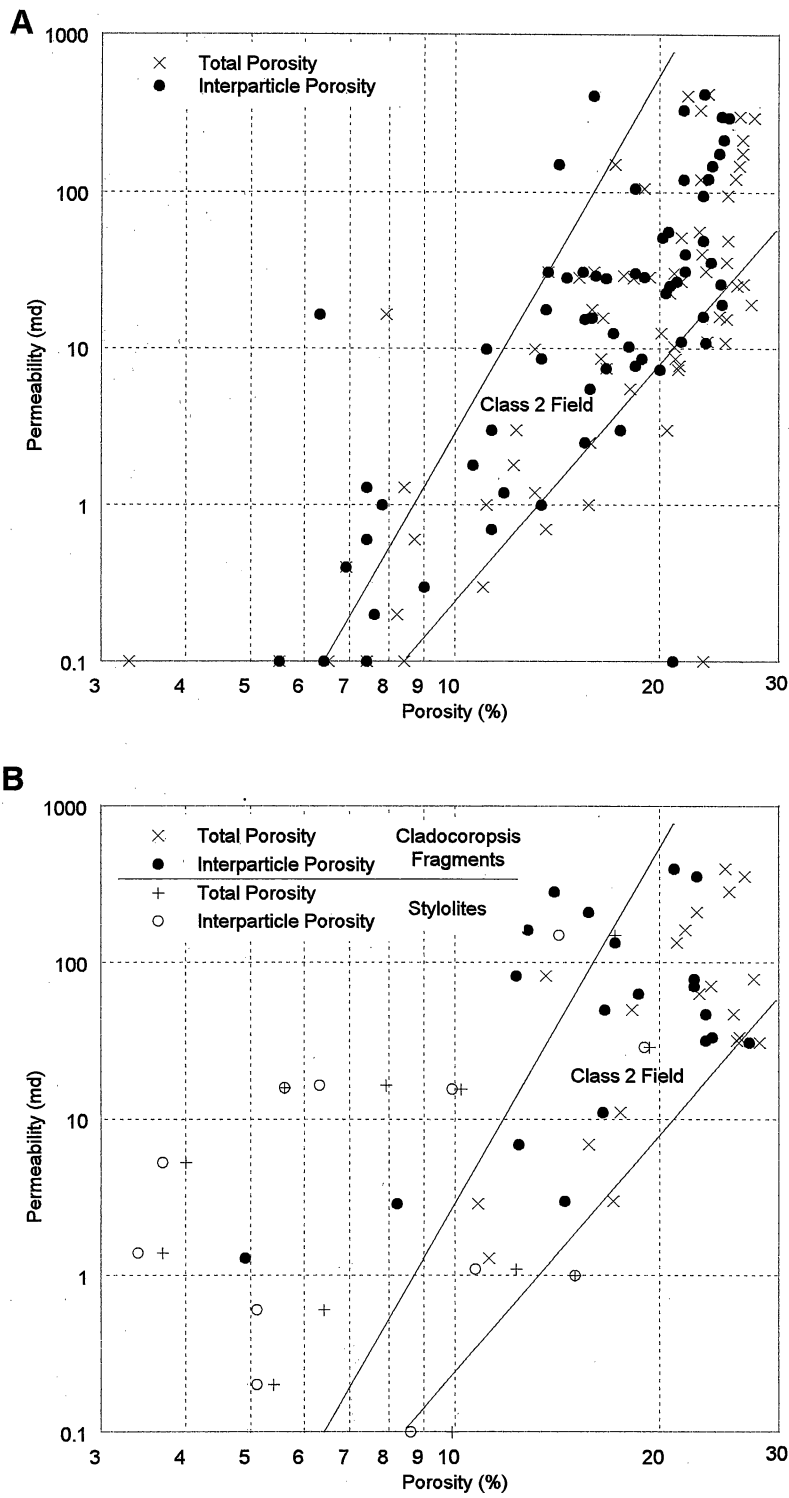


Figure 6. Porosity–permeability cross plot for grain-dominated packstone, showing both total and interparticle porosity. The difference is separate-vug porosity determined by point counting thin sections. (A) Plot of representative samples. These samples have very little vuggy porosity, and most of the samples fall into the petrophysical class 2 field. (B) Plot of samples containing stylolites and large *Cladocoropsis* fragments. Stylolitic and some *Cladocoropsis* samples fall to the left of the class 2 field.

dominated fabrics. Mud content ranges from 5 to 95 percent (fig. 7). Samples having more than 40 to 50 percent mud are mud-dominated fabrics having burrows filled with grain-dominated packstone (fig. 8). Petrophysically these samples belong to the grain-dominated packstone, petrophysical class 2, although depositionally they are most likely quiet-water deposits. Grains are mostly peloids or micritized grains and are difficult to identify. Grain size ranges from 150 to 300 microns, and mud size is less than 20 microns.

Grain-dominated packstones typically have syntaxial cement on echinoderm fragments and no isopachous cement (fig. 8). Interpenetration of grains suggests compaction. In general, these fabrics contain little separate-vug porosity. Intragrain microporosity is most abundant in well HRDH-101 between the depths of 6,555.7 and 6,562.7 ft, although individual samples at other depths have significant amounts of this separate-vug type. In fact, most samples contain at least a few microporous grains; forams in particular appear to be susceptible to leaching and are commonly microporous.

Mud-Dominated Fabrics

Mud-dominated fabrics are (1) mud-dominated packstone that has grains as a supporting fabric but whose intergrain space is filled with micrite, (2) wackestone that has micrite clearly as the supporting fabric, and (3) mudstone that has few observable grains (fig. 9). There are 52 samples of mud-dominated fabrics, 6 of which have been discarded for large *Cladocoropsis* fragments and 7 for stylolites. Of the remaining 35, only 10 are permeable and all but 3 plot in the petrophysical class 3 field (fig. 10). Stylolitic and *Cladocoropsis* samples plot to the left of the class 3 field. Mud-dominated fabrics have little separate-vug pore space. Commonly, however, a few calcisphere or fossil molds are present. In mud-dominated packstones calcisphere molds can be mistaken for interparticle porosity.

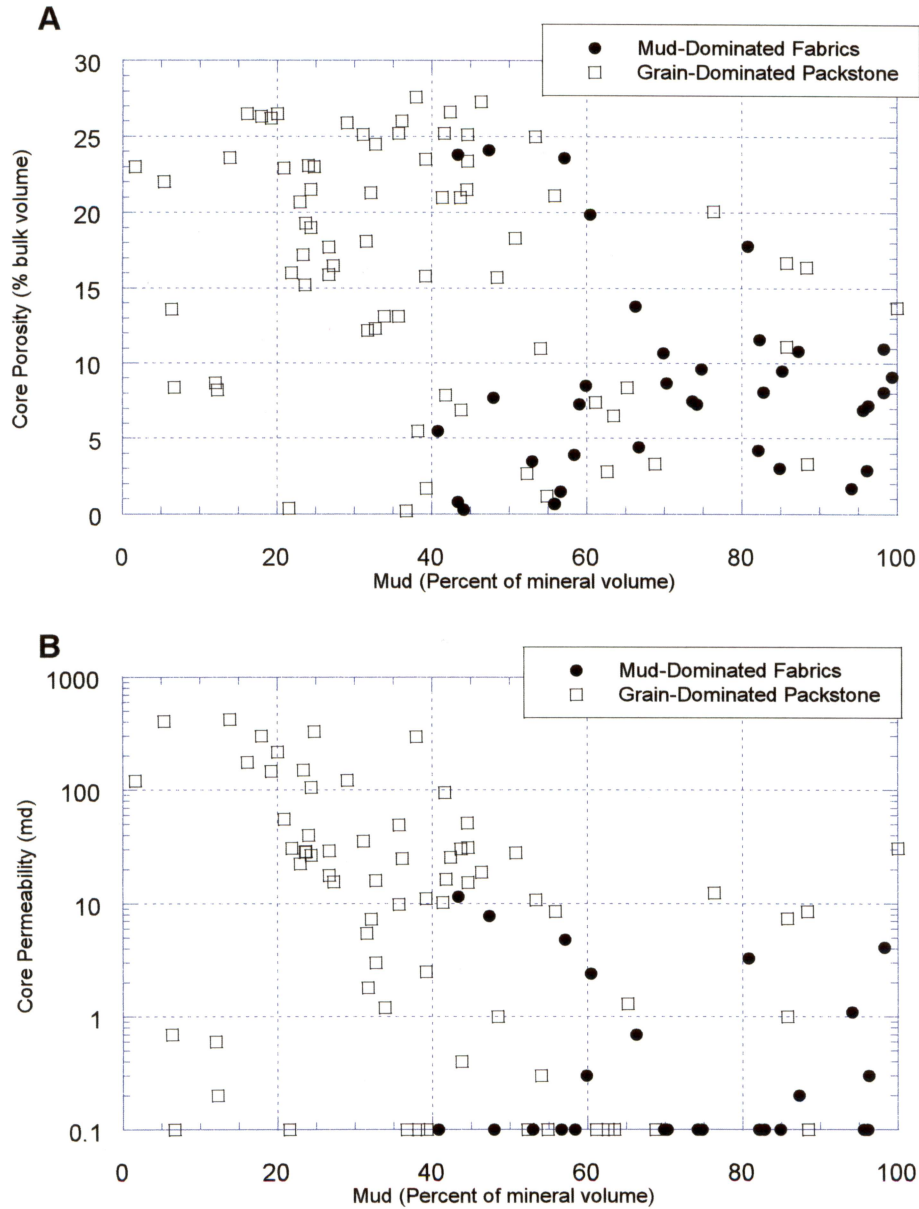


Figure 7. Cross plots of porosity and permeability against mud content for grain-dominated packstones and mud-dominated fabrics. High mud content in some grain-dominated packstones is the result of grain-dominated packstone filling burrows in mud-dominated fabrics. (A) Cross plot of core porosity and mud volume showing a porosity level in grain-dominated packstones different than in mud-dominated fabrics. However, there is little relationship between porosity and mud content within each fabric. (B) Cross plot of permeability and mud volume showing a distinct difference in permeability levels between grain-dominated packstones and mud-dominated fabrics. However, as with porosity, there is little relationship between permeability and mud content within each fabric.

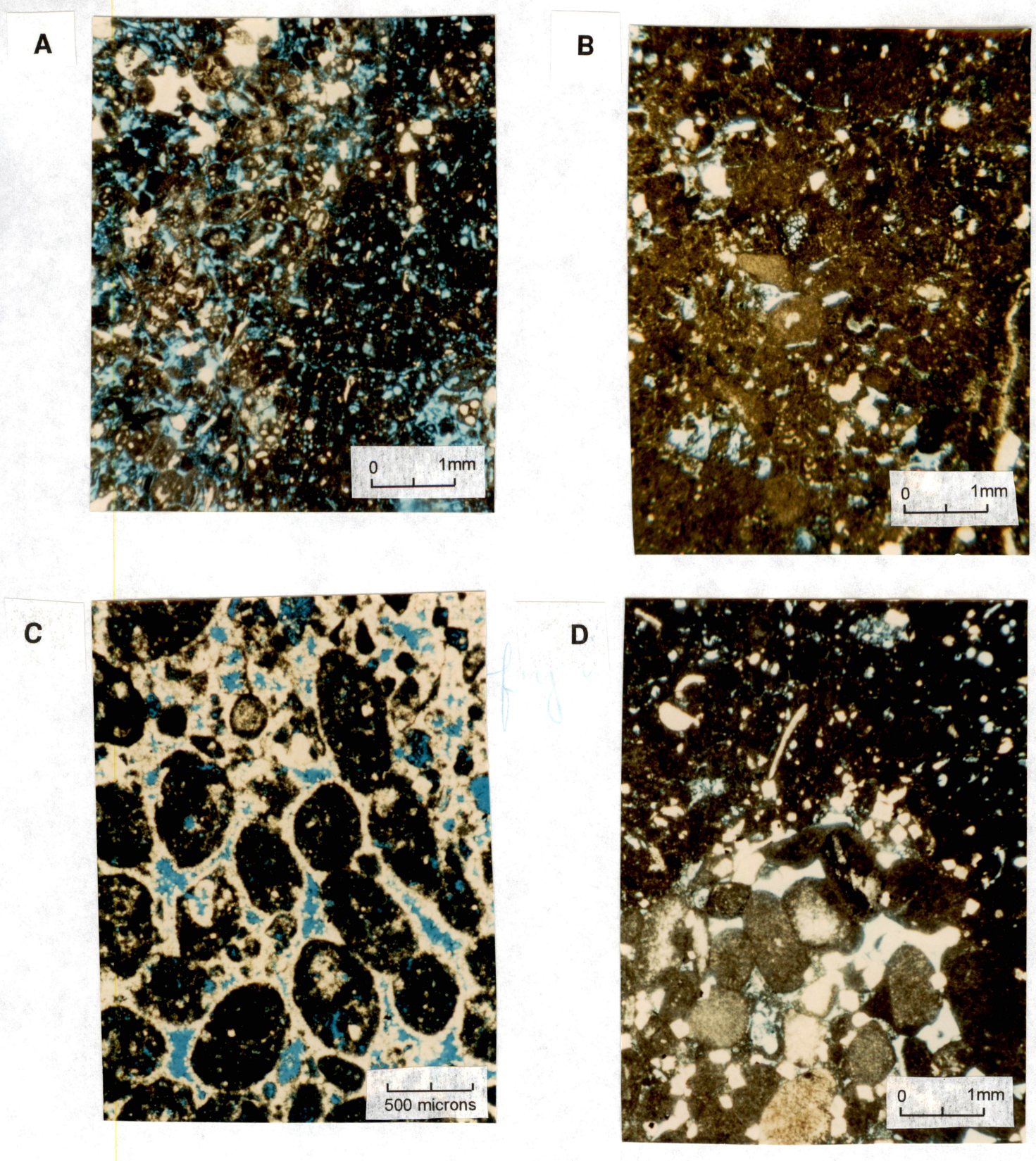
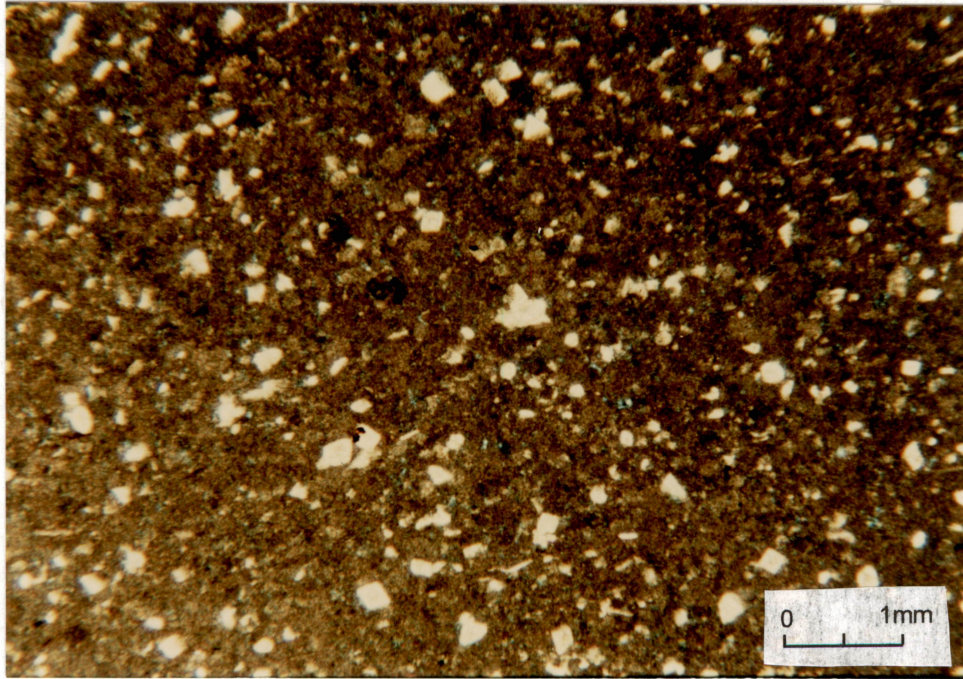


Figure 8. Photomicrographs illustrating range of fabrics classified as grain-dominated packstone. Notice syntaxial cement and grain interpenetration. (A) Grain-dominated packstone having 19 percent mud ($\phi_{ip} = 19\%$, $k = 43$ md). (B) Grain-dominated packstone having 50 percent mud ($\phi_{ip} = 17\%$, $k = 28$ md). (C) Grain-dominated packstone having intragrain microporosity. Twenty-seven percent of the grains are microporous ($\phi_{ip} = 21\%$, $S_{vug} = 5\%$, $k = 28$ md). (D) Wackestone having grain-dominated packstone in burrow ($\phi_{ip} = 8\%$, $k = 1$ md).

A



B

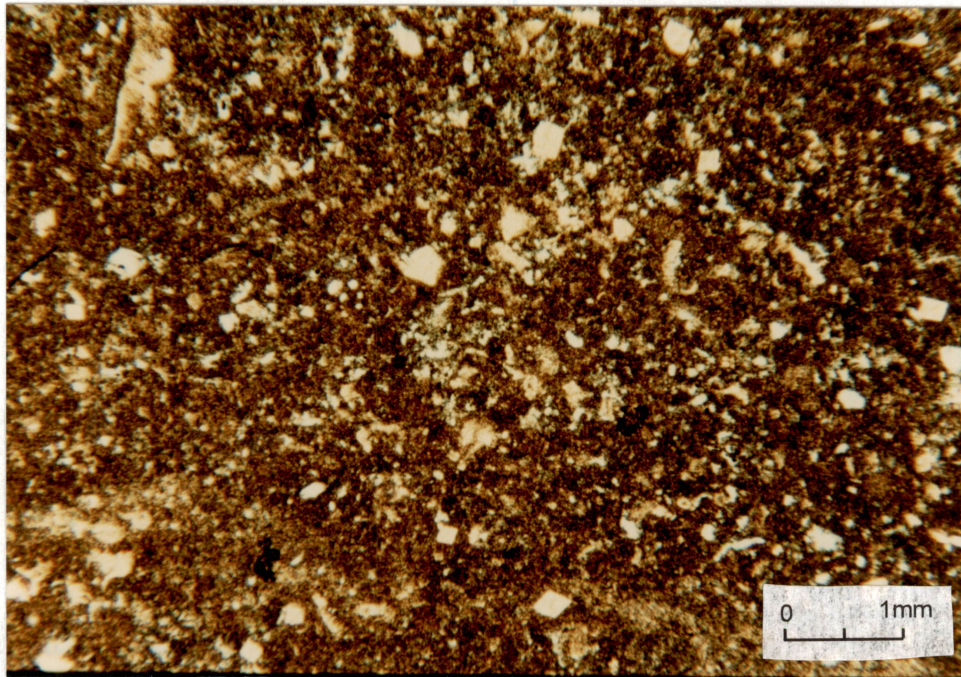
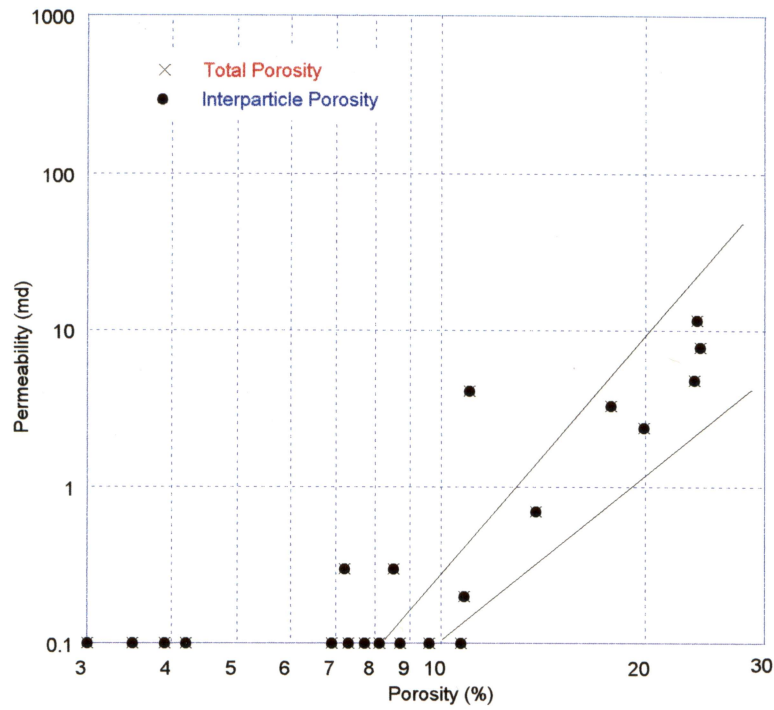


Figure 9. Photomicrographs of permeable mud-dominated fabrics. (A) Wackestone ($\phi_{ip} = 13.8\%$, $k = 0.7$ md). (B) Mud-dominated packstone ($\phi_{ip} = 23\%$, $k = 4.8$ md).

A



B

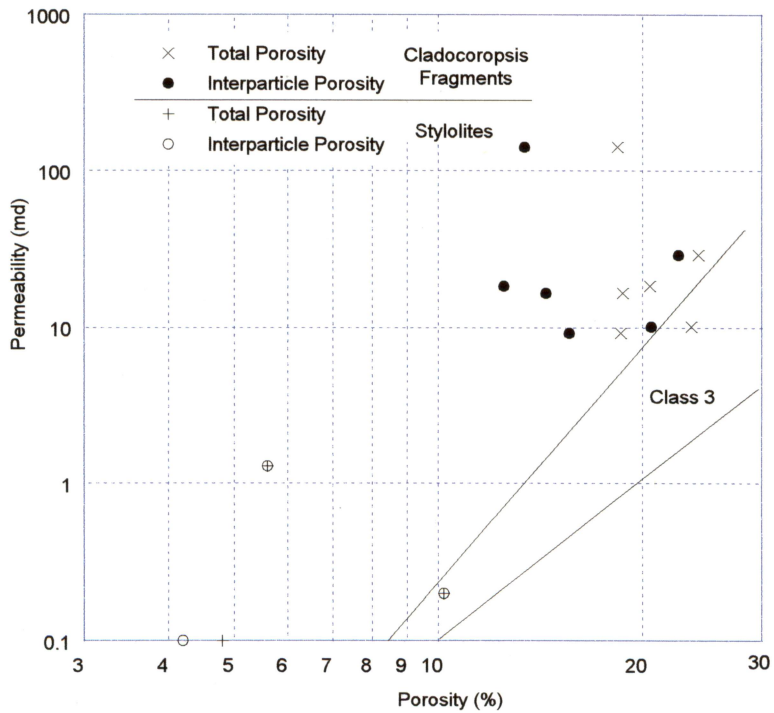


Figure 10. Porosity–permeability cross plot for mud-dominated fabrics, showing both total and interparticle porosity. There is less than 1 percent separate-vug porosity. (A) Plot of representative samples. Most of the samples have less than 0.1 md permeability, and most of the permeable samples fall into the petrophysical class 3 field. (B) Plot of samples having stylolites and large *Cladocoropsis* fragments. All these samples fall to the left of the class 3 field.

DOLOMITIC LIMESTONES (10- TO 80-PERCENT DOLOMITE)

Dolomitic Grain-Dominated Packstones

There are only 27 samples of dolomitic grain-dominated packstone, and all but 4 samples have less than 50 percent dolomite. The dolomite crystal size ranges from 80 to 200 microns. Most of the samples plot within the petrophysical class 2 field (fig. 11). The few low-porosity samples that plot to the left of the class 2 field may be the result of poor measurements. There does not appear to be any relationship between the amount of dolomite and porosity or permeability, suggesting that the partial replacement by large dolomite crystals has not altered the porosity or pore-size distribution (fig. 12).

Dolomitic Mud-Dominated Fabrics

Of the 63 dolomitic mud-dominated samples, 33 have less than 0.1 md permeability. The samples were divided into three groups: 10- to 25-percent, 25- to 50-percent, and 50- to 80-percent dolomite for analysis. There does not appear to be any relationship between the amount of dolomite and porosity. Permeability, however, does appear to have a relationship with amount of dolomite (fig. 13). Permeable samples having 10- to 25-percent dolomite tend to plot in the petrophysical class 3 field, along with mud-dominated fabrics. Permeable samples having 25- to 50-percent dolomite plot in the class 2 field, along with grain-dominated packstones. Permeable samples having 50- to 80-percent dolomite tend to be the most permeable for a given porosity and plot near the class 1 field.

The increase in permeability indicates an increase in pore size with dolomitization. The 33 dense samples, however, show no development of intercrystal porosity with increasing dolomitization. On the other hand, thin-section analysis of the permeability samples suggests an increase in porosity in intercrystal mud and dissolution of the intercrystal mud to form intercrystal

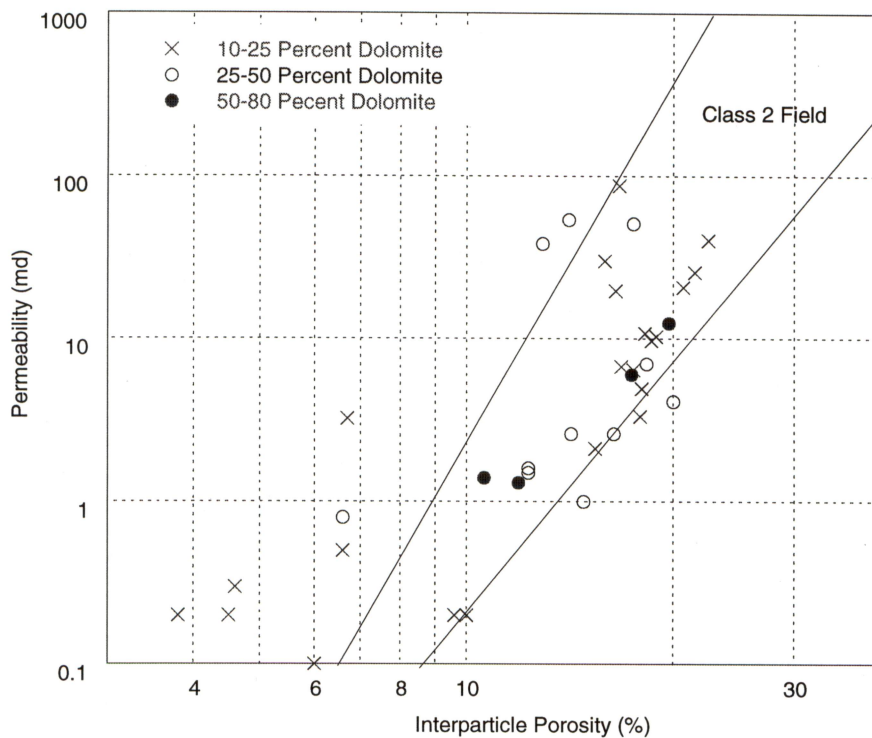


Figure 11. Porosity-permeability cross plot for dolomitic grain-dominated packstone (10 to 80 percent dolomite). Dolomite percentage is plotted in three groups, showing little relationship between dolomite percentage and porosity or permeability. Most samples plot in the class 2 field. Most of the low-porosity, high-permeability samples are wackestones having grain-dominated packstone in burrows, and the permeability will depend upon the volume and distribution of the burrows within the core plug.

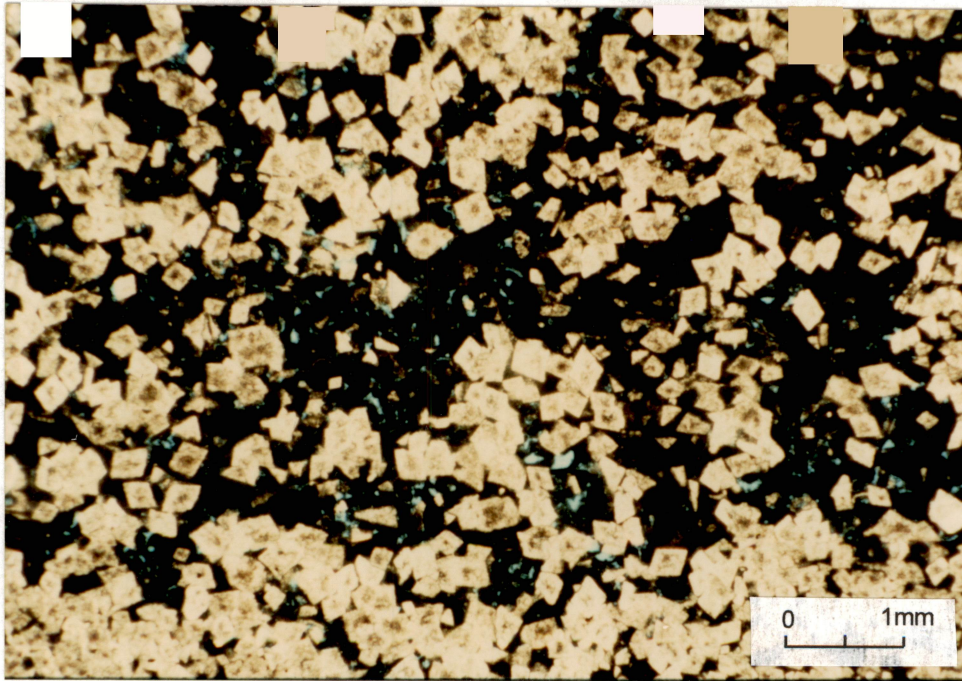
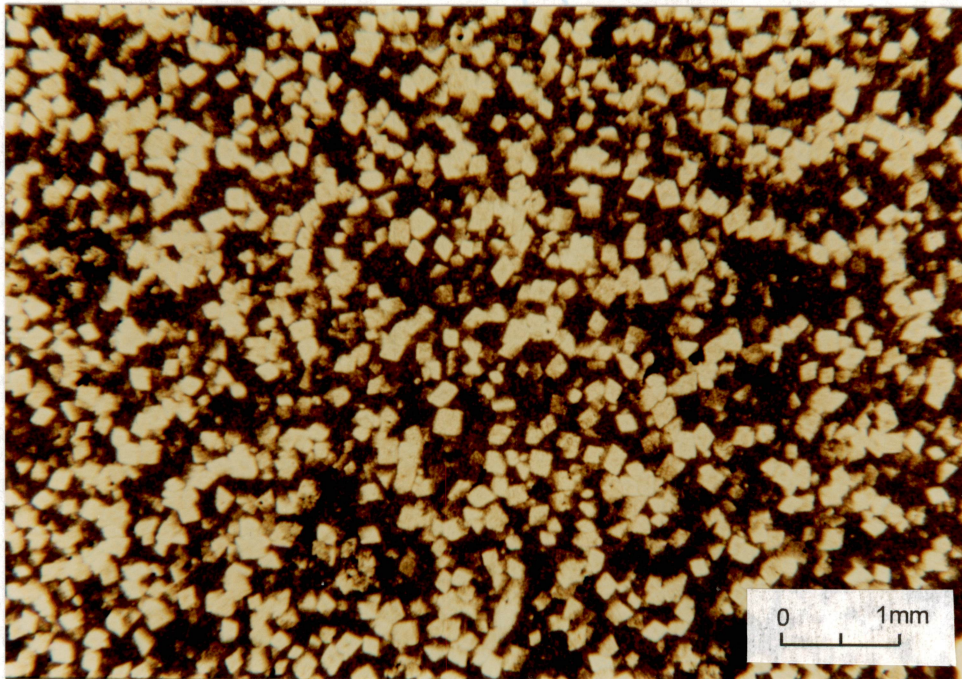
A**B**

Figure 12. Photomicrographs of dolomitic limestones. (A) Dolomitic grain-dominated packstone having 54 percent dolomite. Dolomite crystal size is 140 microns. ($\phi_{ip} = 17.4\%$, $k = 6.0$ md). (B) Dolomitic wackestone having 40 percent dolomite. Dolomite crystal size is 80 microns. ($\phi_{ip} = 5\%$, $k = <0.1$ md).

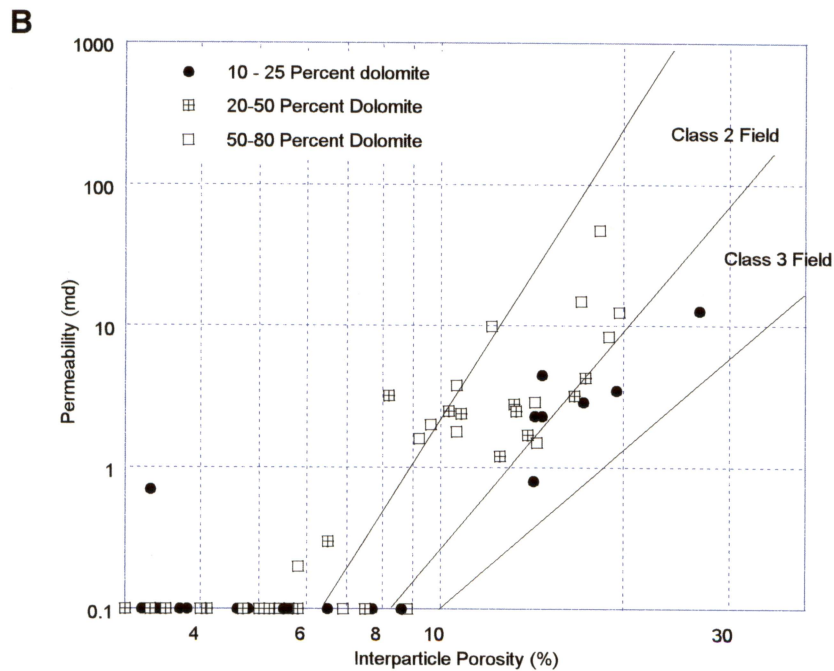
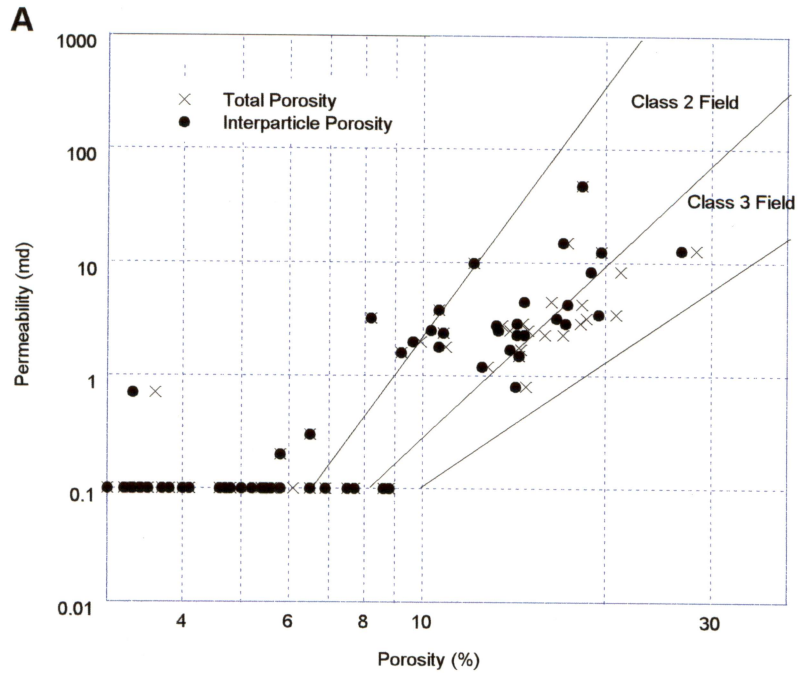


Figure 13. Porosity-permeability cross plot for dolomitic mud-dominated fabrics (10 to 80 percent dolomite). (A) Plot of total and interparticle porosity, showing little separate-vug porosity and most permeable samples plotting in class 2 field instead of in the class 3 field. (B) Plot showing dolomite percentage in three groups, which illustrates an apparent increase in permeability with increasing amount of dolomite. Samples having 10 to 25 percent dolomite plot in class 3 field, and the rest plot in the class 2 field.

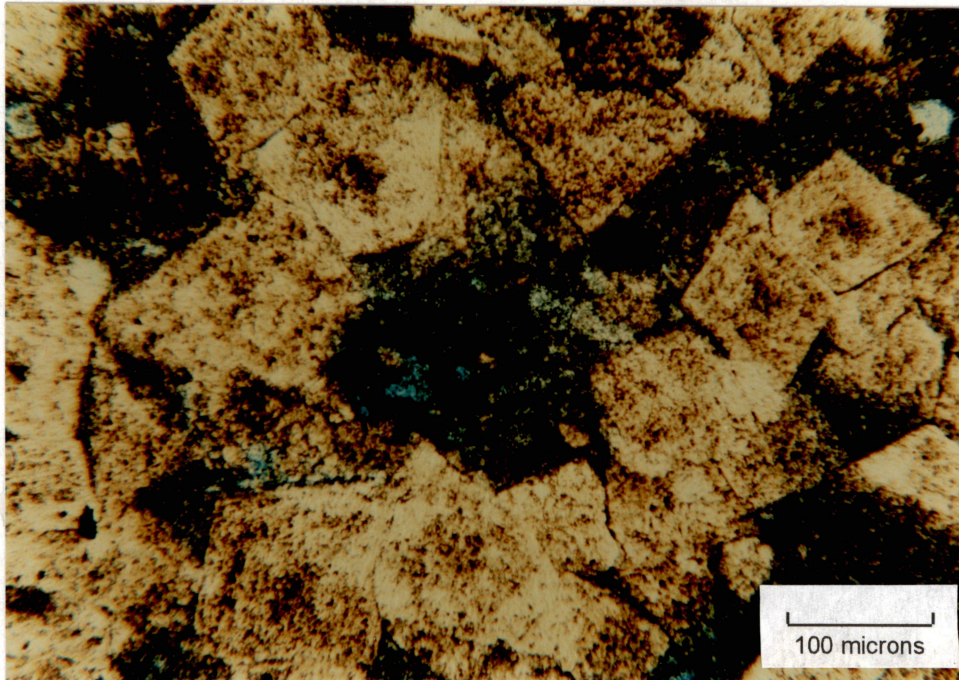
pore space. For example, figure 14A shows 71-percent dolomite and porous intercrystal mud. Assuming that the dolomite crystals are nonporous, the measured porosity must be within the mud fraction. The measured porosity is 17 percent, and a simple calculation shows that the mud fraction has a porosity of 58 percent. The high porosity value equates to a larger pore size than found in a mud-dominated fabric having 17-percent interparticle porosity. Figure 14B illustrates a thin section where intercrystal mud has been partially dissolved to create intercrystal porosity space. It is possible that the increase in permeability with increasing mud content that Powers (1962) observed, is an increase in pore size with dolomitization rather than an increase in porosity.

DOLOSTONE

Dolostone samples are characterized by dolomite crystals that are more than 100 microns in size. Most are permeable and all plot in or to the left of the class 1 grainstone field (fig. 15). Porosity is intercrystal between dolomite crystals, ranging from 100 to 500 microns; intercrystal porosity ranges from 3 to 25 percent (fig. 16). Some samples have bimodal dolomite-size distributions. These samples have patchy areas of relatively tight, coarse (250 to 350 mm), cloudy dolomite crystals within porous areas of medium (150 to 250 mm) dolomite crystals having cloudy centers and clear rims. Several thin sections contain abundant skeletal dolomite. Other minerals found in the dolomite are small amounts of anhydrite in the form of laths, chert, and a green clay mineral (probably chlorite). Samples that have abundant chert or green clay were discarded from the data set.

Samples were divided into three groups according to crystal size: 100 to 200 microns, 200 to 300 microns, and 300 to 500 microns. The porosity-permeability cross plot shows that permeability increases as dolomite crystal size increases (fig. 15B). The plot also shows that a number of samples plot to the left of the petrophysical class 1 field. Most of these dolostones have dolomite crystals larger than 200 microns, indicating that the upper limit of class 1 should be moved left to accommodate these samples, as shown in figure 15B.

A



B

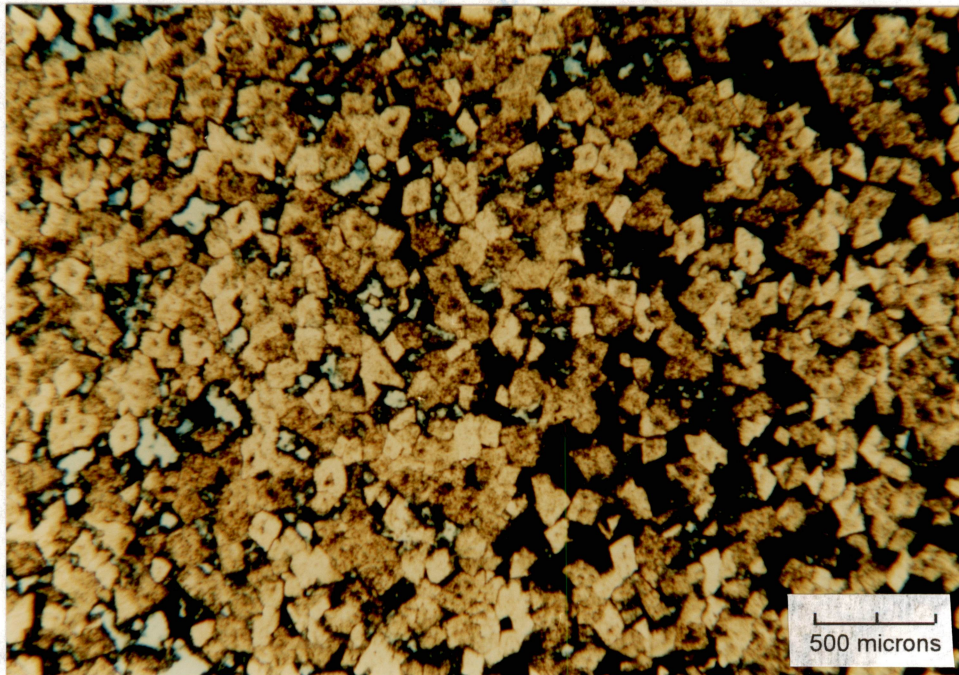


Figure 14. Photomicrographs of dolomitic wackestones illustrating the development of intercrystal porosity. (A) Sample showing increase in porosity in intercrystal mud ($\phi_{ip} = 17\%$, $k = 15$ md). (B) Sample showing dissolution of intercrystal mud to form intercrystal pore space ($\phi_{ip} = 18\%$, $k = 47$ md).

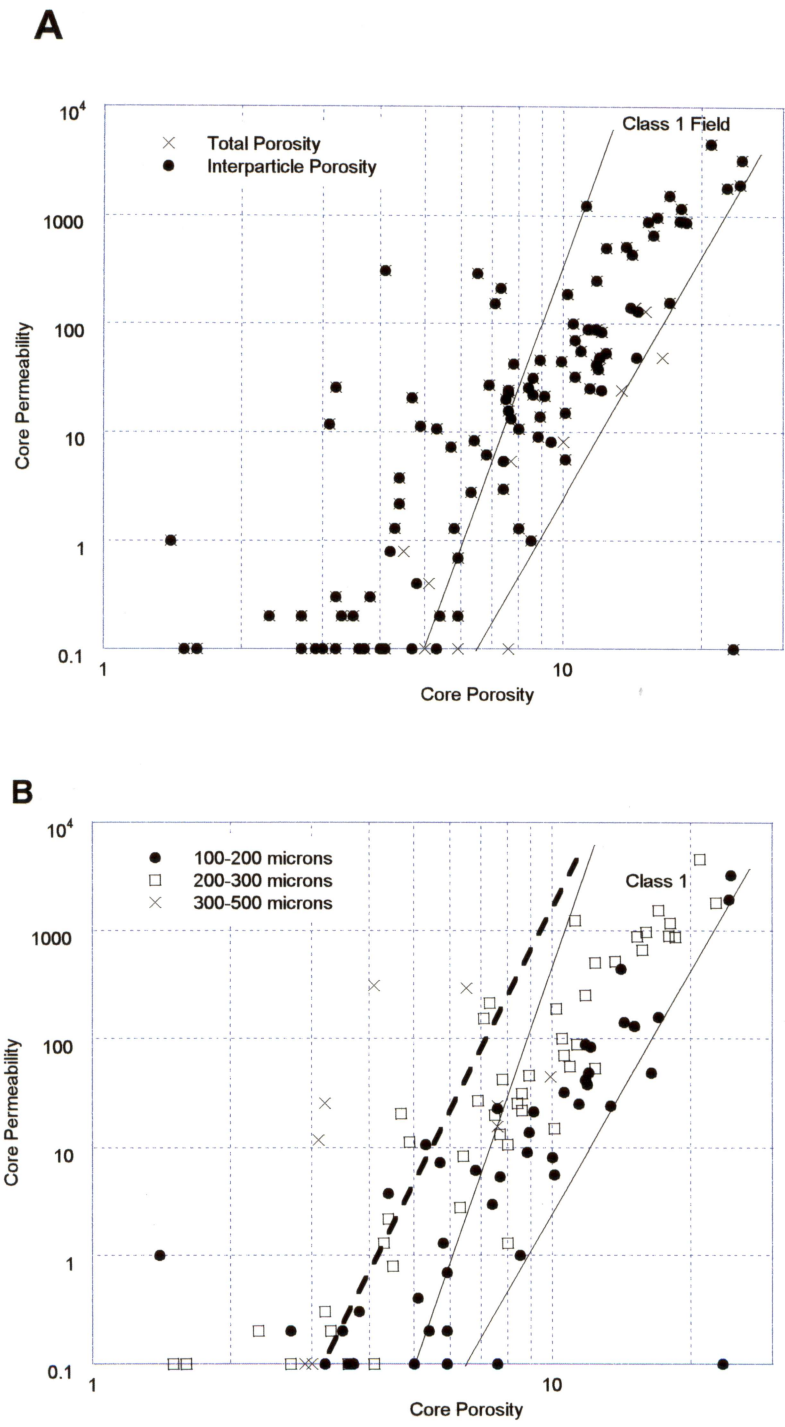
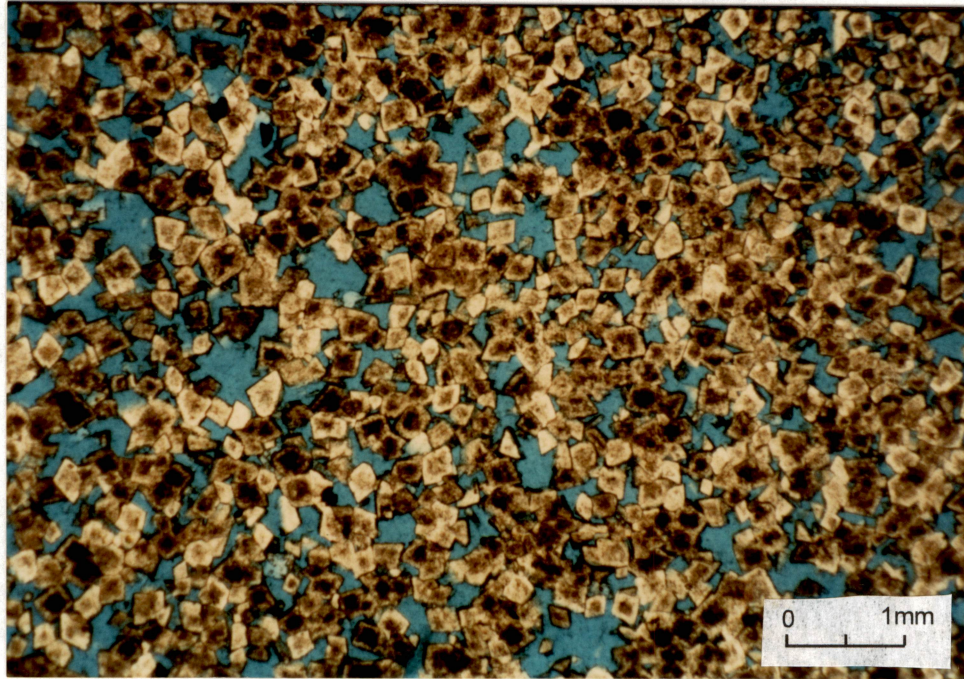


Figure 15. Porosity–permeability cross plot for dolostones. (A) Plot of total and interparticle porosity showing little separate-vug porosity. Most permeable samples plot in the class 1 field, but many plot to the left of the class 1 field. (B) Plot having dolomite crystal size in three groups, which shows an apparent increase in permeability with increasing dolomite crystal size. The class 1 field must be enlarged to accommodate the range of dolomite crystal sizes of from 100 to 300 microns.

A



B

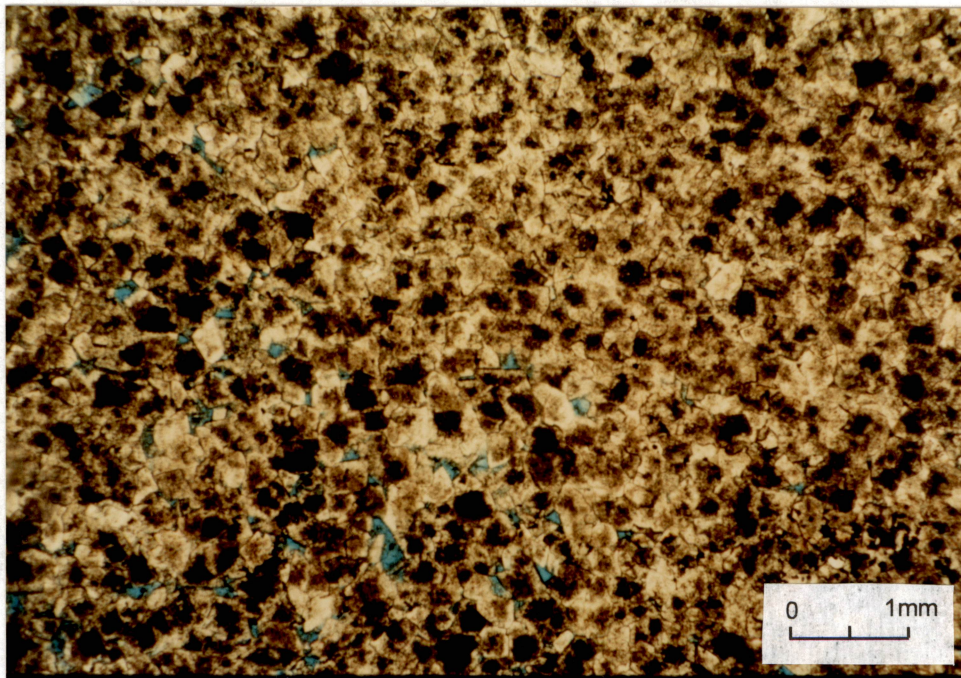


Figure 16. Photomicrographs of dolostone. The precursor fabric cannot be determined. (A) Intercrystal porosity in dolostone having 200-micron crystals. ($\phi_{ip} = 24\%$, $k = 3,279$ md). (B) Dense dolostone having 200-micron crystals ($\phi_{ip} = 3\%$, $k = <0.1$ md).

POROSITY-PERMEABILITY TRANSFORMS

Analysis of thin section and core data demonstrates that rock fabrics can be grouped into petrophysical fields according to porosity and permeability (fig. 17). Grainstones and large crystal dolostones fall within the petrophysical class 1 field of Lucia (1995). The permeability of the dolostones increases with increasing crystal size. The class 1 field is enlarged to include dolostones having crystal sizes larger than 200 microns. Grain-dominated and dolomitic grain-dominated packstones plot within the petrophysical class 2 field of Lucia (1995). Dolomitic mud-dominated fabrics having more than 25 percent dolomite also fall in the class 2 field because of the increase in pore size related to the dolomitization process. Mud-dominated fabrics having less than 25 percent dolomite are mostly dense but, when permeable, plot in the petrophysical class 3 field.

The three generic rock-fabric-specific porosity-permeability transforms developed by Lucia (1995) can be used to calculate permeability for this suite of rocks. The permeability of the dolomites, however, may be understated because the class 1 transform does not account for the larger-than-200-micron crystal size. Although fabrics are divided into three petrophysical classes, in nature there is no boundary between the classes. Instead, there is a continuum from mudstone to grainstone and from 5- μm mud-dominated dolostones to 500- μm mud-dominated dolostones. Therefore, there is also a complete continuum of rock-fabric-specific porosity-permeability transforms.

To model such a continuum, the boundaries of each petrophysical class are assigned a value (0.5, 1.5, 2.5, and 4) (fig. 18) and porosity-permeability transforms are generated. An equation relating permeability to a continuum of petrophysical classes and interparticle porosity is developed by multiple linear regression. The resulting global transform is

$$\text{Log}(k) = (A + B \times \text{Log}(\text{Class})) + (C + D \times \text{Log}(\text{Class})) \times \text{Log}(\Phi_{ip}),$$

where

$$A = 9.7982,$$

$$B = 12.0838,$$

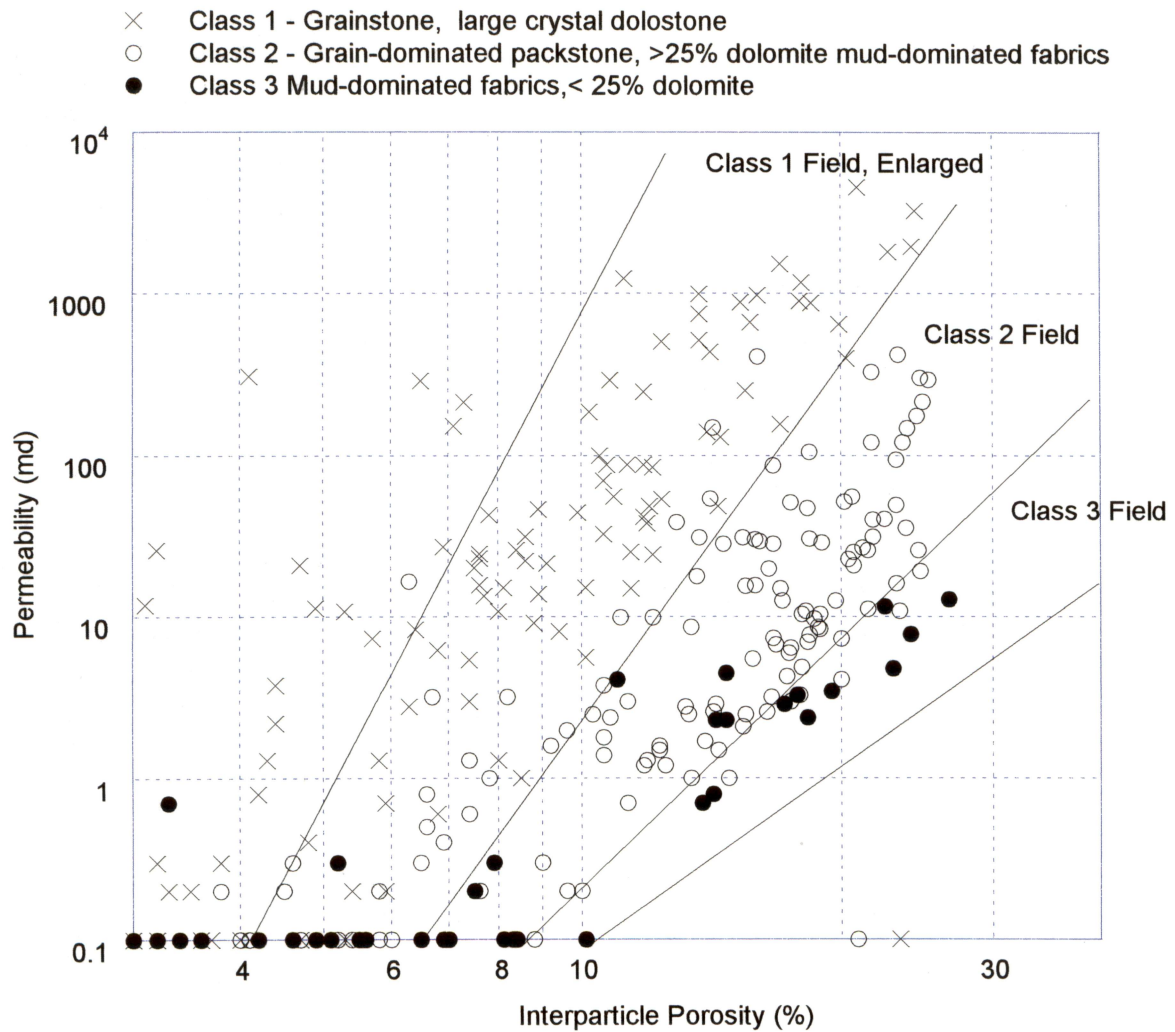


Figure 17. Porosity–permeability cross plot of all representative samples showing rock-fabric petrophysical classes.

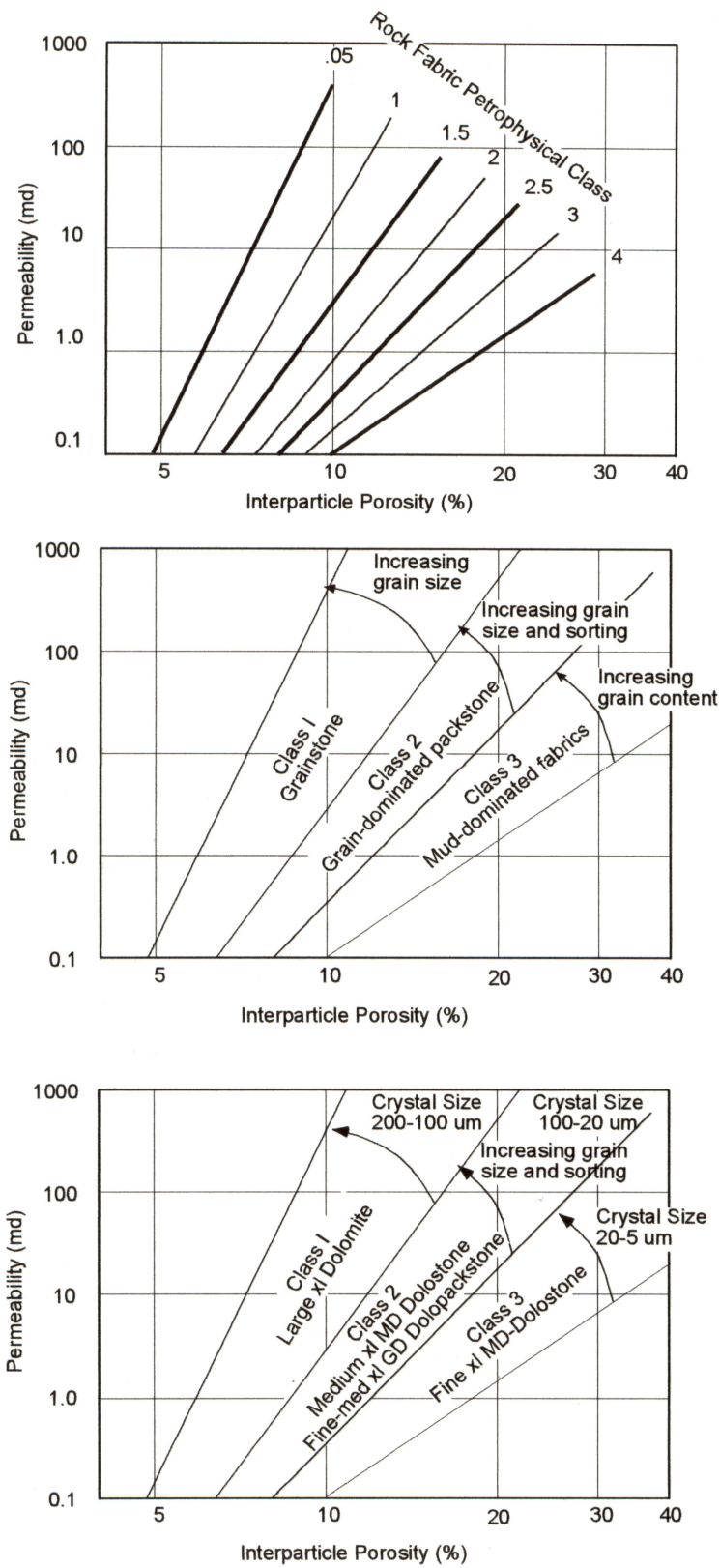


Figure 18. Continuum of rock fabrics and associated porosity–permeability transforms. (A) Rock-fabric petrophysical classes ranging from 0.5 to 4 defined by class-average and class-boundary porosity–permeability transforms. (B) Fabric continuum in nonvuggy limestone. (C) Fabric continuum in nonvuggy dolostone.

$$C = 8.6711,$$

$$D = 8.2065,$$

and

Class = Rock-fabric petrophysical class ranging from 0.5 to 4, and

Φ_{ip} = Fractional interparticle porosity.

Mud-dominated limestones and fine crystalline mud-dominated dolostones occupy classes from 4 to 2.5 (fig. 18a, b). The class number decreases with increasing dolomite crystal size from 5 to 20 microns in mud-dominated dolostones and increasing grains in mud-dominated limestones. Grain-dominated packstones, fine to medium crystalline grain-dominated dolopackstones, and medium crystalline mud-dominated dolostones occupy classes from 2.5 to 1.5 (fig. 18a, b). The class value decreases with increasing dolomite crystal size from 20 to 100 microns in mud-dominated dolostones and with decreasing amounts of intergrain micrite, as well as increasing grain size in grain-dominated packstones and fine to medium crystalline grain-dominated dolopackstones. Grainstones, dolograinstones, and large crystalline dolostones occupy classes 1.5 to 0.5 (fig. 18a, b). Class value decreases with increasing grain size from 100 to 500 microns, and dolomite crystal size from 100 to 200 microns.

PERMEABILITY FROM WIRELINE LOGS

Approach

No wireline log measures permeability. Instead, permeability is estimated according to empirical relationships between wireline log values and permeability, most notably porosity. In the rock-fabric method, rock fabrics are determined by porosity, water saturation, and reservoir-height cross plots. Rock-fabric-specific porosity-permeability transforms are then used to estimate permeability. Permeability, however, has been shown to be related to interparticle porosity, not total porosity (Lucia, 1983). Separate-vug porosity must therefore be determined and subtracted

from total porosity before permeability can be estimated. Acoustic-porosity cross plots are used to make this determination.

Calibrating log data with core data and rock-fabric descriptions requires matching core depths and log depths as closely as possible. Although no depth shift was made in well 106, a large adjustment was made in well 101. Matching core data with log data exactly is nearly impossible and accounts for much of the imprecision that results from comparing core and log data. In addition to matching core and log depths, there is a large scaling problem between wireline-log measurements, core measurements, and thin-section descriptions. Wireline logs average data over intervals of several feet, whereas core data are measured on core plugs or 6-inch whole core samples, and thin-section descriptions are made on 1-inch \times 30-micron slices of core. In order to scale rock-fabric descriptions to wireline logs, it is necessary to find intervals of uniform fabric covering more than 3 ft.

Calculation of Interparticle Porosity

Interparticle porosity is calculated by subtracting separate-vug porosity from total porosity. Total porosity can be calculated from neutron, density, and acoustic logs by means of various algorithms. In this study, flame porosity values provided by Aramco were used. Separate-vug porosity is estimated from cross plots of transit time (from acoustic logs) and total porosity. The assumption is that porosity and transit time follow the Wyllie time-average curve if separate-vug porosity is constant. Relationships for limestones and for anhydritic dolomite have been derived (Wang and Lucia, 1993). These relationships have the form

$$S_{vug} = 10^a + b(\Delta t + 141.5 \times \phi),$$

or

$$S_{vug} = A \times e^{B(\Delta t + 141.5 \times \phi)}.$$

For limestones,

$$A = 13,406, \text{ and}$$

$$B = -0.2987.$$

For anhydritic dolomite,

$$A = 8,920, \text{ and}$$

$$B = -0.3254.$$

The slopes are very similar, and the intercept varies with lithology. The lithology effect is expressed in the Δt term at zero porosity. The Arab D limestone has a Δt of 48 $\mu\text{sec}/\text{ft}$ at zero porosity (fig. 19), which is characteristic of most limestones, and the constants for limestone are used to calculate separate-vug porosity. The dolostone has little separate-vug porosity. Assuming that the dolostone has an average separate-vug porosity of 0.01, the Δt at zero porosity at 0.01 is 40 $\mu\text{sec}/\text{ft}$ (fig. 19). Assuming a constant slope (B constant) (fig. 19), an intercept value of 4,953 is calculated. The constants for calculating separate-vug porosity in dolostone are, for Arab D dolomite (no anhydrite),

$$A = 4,953, \text{ and}$$

$$B = -0.3254.$$

The lithology of the Arab D is variable, and a relationship between the mineral fraction that is dolomite and transit time, porosity, and separate-vug porosity was developed:

$$S_{\text{vug}} = (13,406 - D_f \times 8,753) \times e^{-0.32(\Delta t + 141.5 \times \phi)},$$

where

$$D_f = \text{dolomite fraction.}$$

An algorithm using neutron and density curves determined dolomite percentages.

Comparisons of calculated and core separate-vug porosity values according to vertical profiles show a good correlation (fig. 20). Spikes in the thin-section data are due partly to small-scale variability averaged out by wireline logs. In well 106, deviations between core and calculated separate vugs are thought to be a scaling problem. In well 101, intervals of high separate-vug porosity from log calculation may be touching-vug horizons. The flow meter from well 101 shows 60 percent of the flow from a 10-ft interval (6,575 to 6,585) and an additional 20 percent from the interval 6,585 to 6,610. There are no core data from this interval. The interval does, however, lie

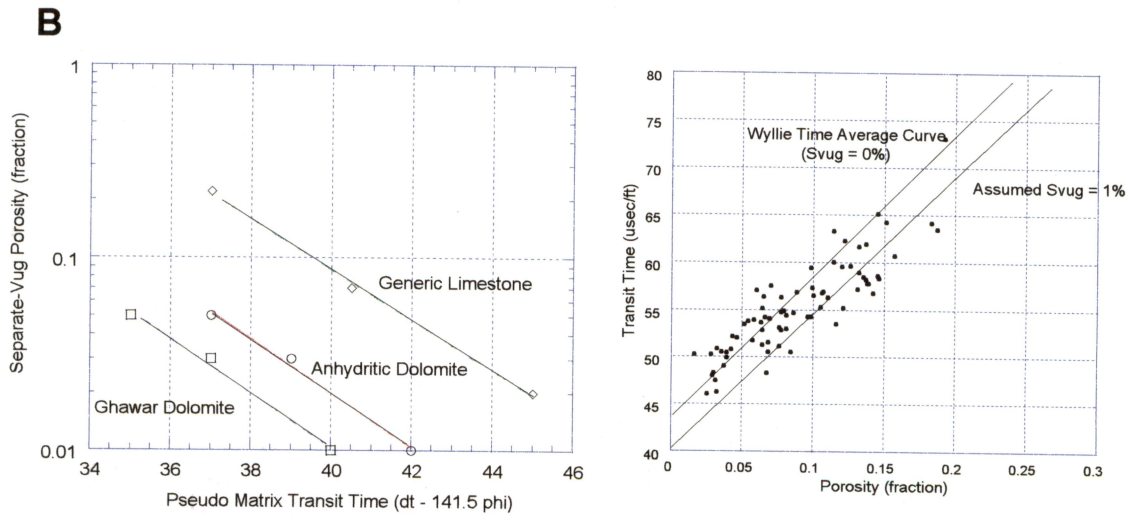
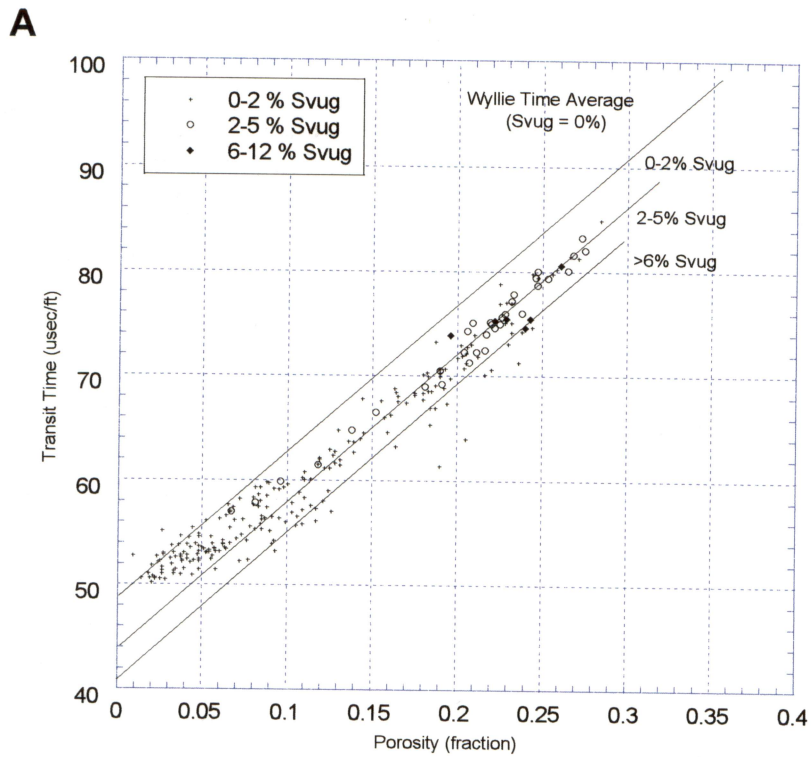


Figure 19. Acoustic, porosity, separate-vug relations from wells HRD 101 and 106. (A) Cross plot of transit time and porosity for limestones and dolomites showing a Wyllie time-average curve having a matrix Δt of 48 $\mu\text{s}/\text{ft}$ for limestone having no Svug porosity and a matrix Δt of 45 $\mu\text{s}/\text{ft}$ for dolomite, assuming an average of 0.01 Svug porosity for the dolomite results in a pseudomatrix Δt of 40 $\mu\text{s}/\text{ft}$. (B) Cross plot of pseudomatrix Δt and separate-vug porosity for limestone, anhydritic dolostone, and Ghawar dolostone.

HRDH 101

HRDH 106

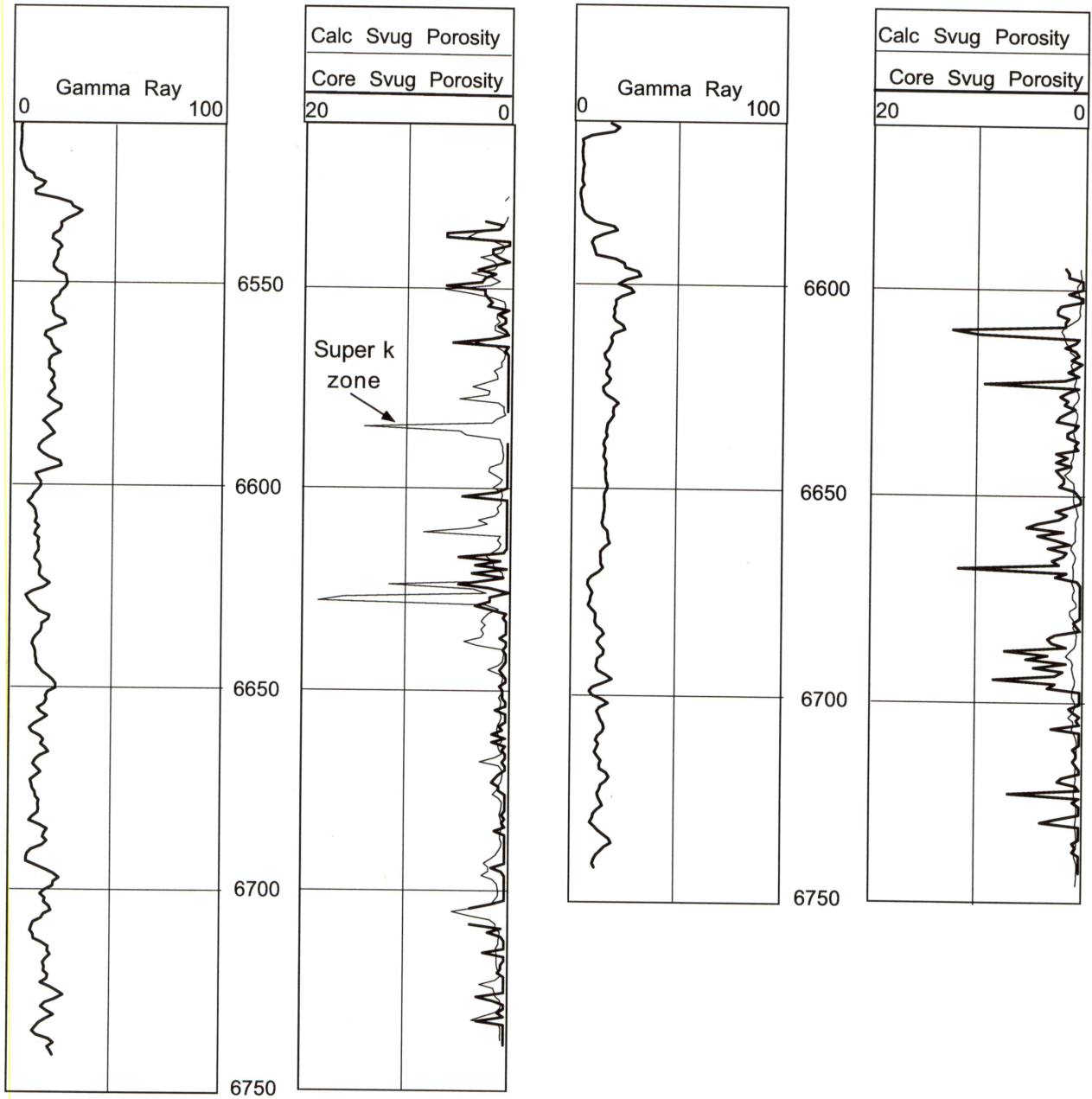


Figure 20. Comparison of separate-vug porosity from logs and thin sections in wells HRDH 101 and 106. High log-calculated separate vugs in well 101 are thought to be caused by touching-vug pore systems. In well 106, the spikes for core descriptions are thought to be caused by small-scale heterogeneity.

within a zone of large crystal dolostone, the porosity log calculates to as much as 30-percent porosity, and the caliper shows a slight hole enlargement. These observations all suggest the presence of a touching-vug pore system composed of enlarged fractures and small cavities. The high separate-vug porosity values in well 101 are therefore incorrect and reflect acoustic response to fractures and caverns.

Determination of Rock-Fabric Petrophysical Class

Rock-fabric petrophysical class is determined from cross plots of water saturation and porosity. Wells 101 and 106 are sufficiently high above the free-water level that reservoir height can be ignored. Flame porosity and water-saturation values provided by Aramco were used in this analysis. Only fabrics having more than 0.1 md permeability were used to calibrate the cross plot, and only that area of the cross plot having greater than 5-percent porosity was used in the analysis. Large crystal dolostone and grainstone (class 1) form a field characterized by low water saturation, and the coarser dolostones tend to have lower water saturations. The lower limit of this field was assigned a class of 0.5 and the upper limit a class of 1.5 (fig. 21). Grain-dominated packstones and mud-dominated fabrics that have 25- to 80-percent dolomite form a prominent trend and contain a majority of the data points. This prominent trend was assigned a class of 2 (fig. 21). There are only a few permeable mud-dominated fabrics, and in general they are too thin for log calibration. However, two intervals of permeable mud-dominated fabrics were large enough to be used to calibrate the cross plot: 6,691 to 6,696 in well 106 and 6,702 to 6,705 in well 101. The boundary between the grain-dominated packstones and mud-dominated fabrics was assigned class 2.5, the class 3 line was drawn through a small group of mud-dominated fabrics, and the upper limit of the mud-dominated fabrics (class 4) was spaced above the group (fig. 21). A relationship between rock-fabric petrophysical class, water saturation, and porosity was developed by multilinear regression on the equations for the class boundaries. Calculated and core rock-fabric petrophysical classes show a good correlation:

Rock-Fabric/Petrophysical Class Saturation - Porosity Relationship

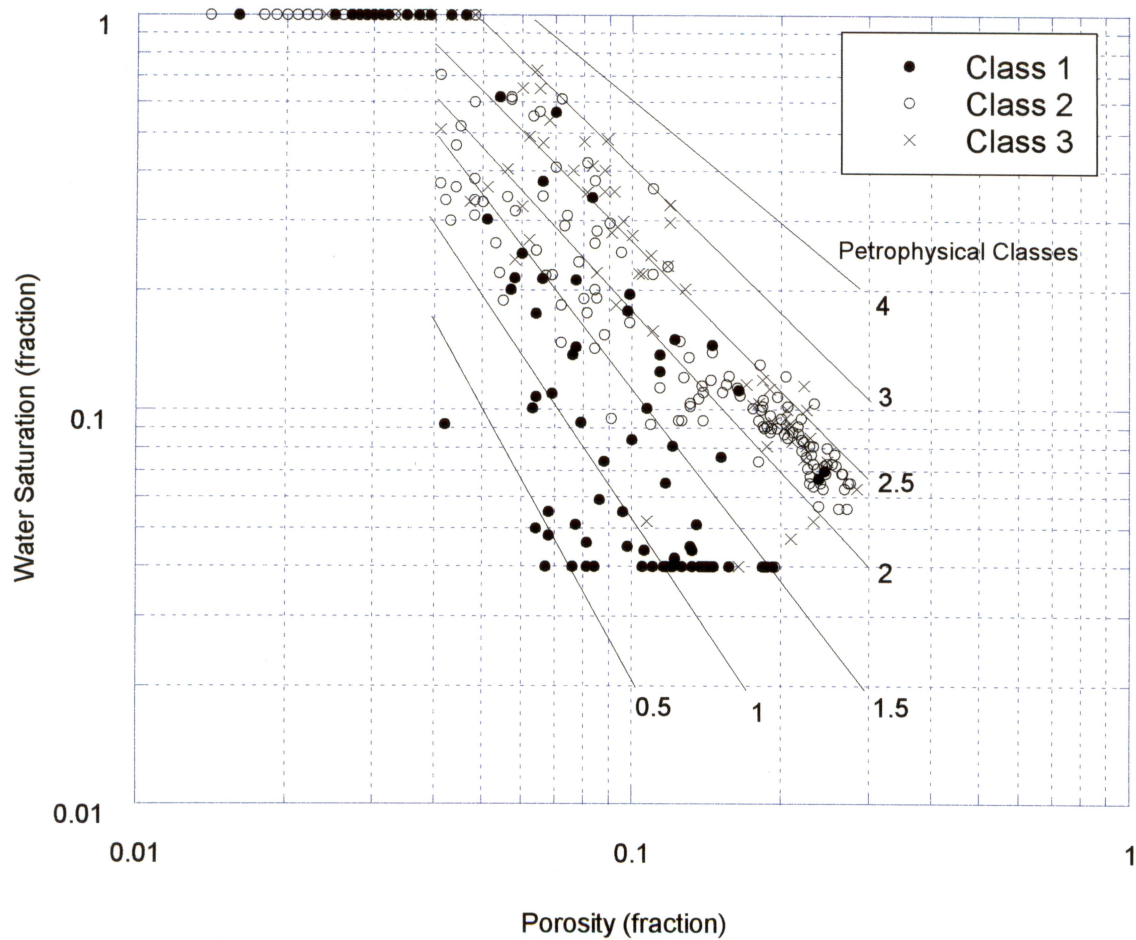


Figure 21. Cross plot of porosity and water saturation showing rock-fabric petrophysical classes. The curves are used to construct an equation relating saturation and porosity to petrophysical class for input into the global, interparticle-porosity, permeability transform equation.

$$\text{Log (Class)} = (A + B \log(\phi) + \log(S_w)) / (C + D \log(\phi)),$$

where

Class = Rock-fabric petrophysical class ranging from 0.5 to 4

$$A = 3.1107$$

$$B = 1.8834$$

$$C = 3.0634$$

$$D = 1.4045$$

The use of this equation is limited to permeable intervals and porosity above 5 percent. In most cases, because samples with less than 5-percent porosity are mud-dominated fabrics or petrophysical class 3, log readings of less than 5-percent porosity were arbitrarily given a petrophysical class of 3.

Calculated and core rock-fabric petrophysical classes show a good correlation. The calculated classes are a continuum, whereas the core classes are specific. The calculated classes in general fall within the range of the specific classes from thin-section description. The continuous profile from log calculations shows interesting detailed vertical patterns not seen in thin-section descriptions. How the patterns relate to rock-fabric successions has not been determined.

In well 101 (fig. 22) there is a major discrepancy around 6,580 that is probably due to the presence of a touching-vug pore system composed of enlarged fractures and small cavities. Water-saturation values are higher than expected for this interval, and the higher water saturation results in a lower petrophysical class than expected. An m value of 1 is required to obtain reasonable water-saturation values. Touching-vug pore systems are not amenable to this type of analysis.

In well 106 (fig. 23) the correlation between log-calculated and thin-section rock fabrics is very good. The two principal dolomite intervals (class 1) are identified, and the upper interval of grain-dominated packstone and the lower interval of alternating grain-dominated packstone and mud-dominated fabrics are clear. The thin, mud-dominated intervals are averaged out of the wireline-log calculations.

HRDH 101

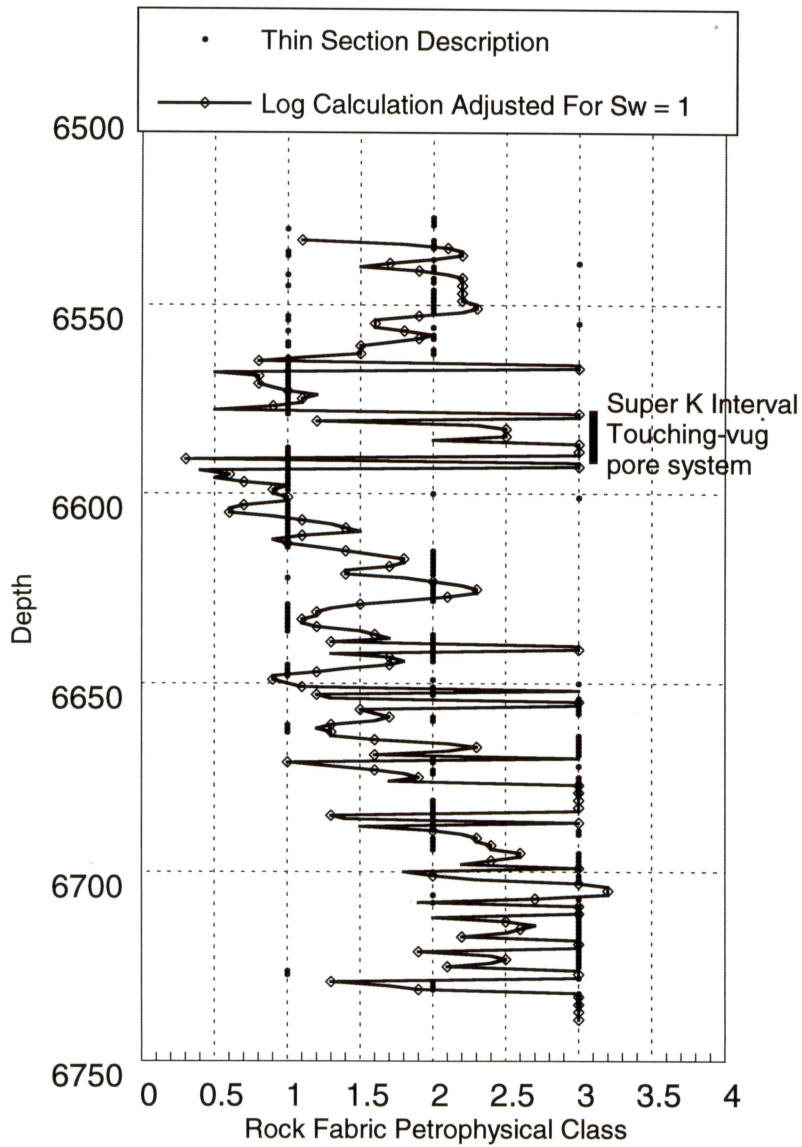


Figure 22. Comparison of petrophysical classes from logs and thin sections for well HRDH 101. Petrophysical classes are incorrectly calculated in the super-k interval because water saturation is incorrectly calculated.

HRDH 106

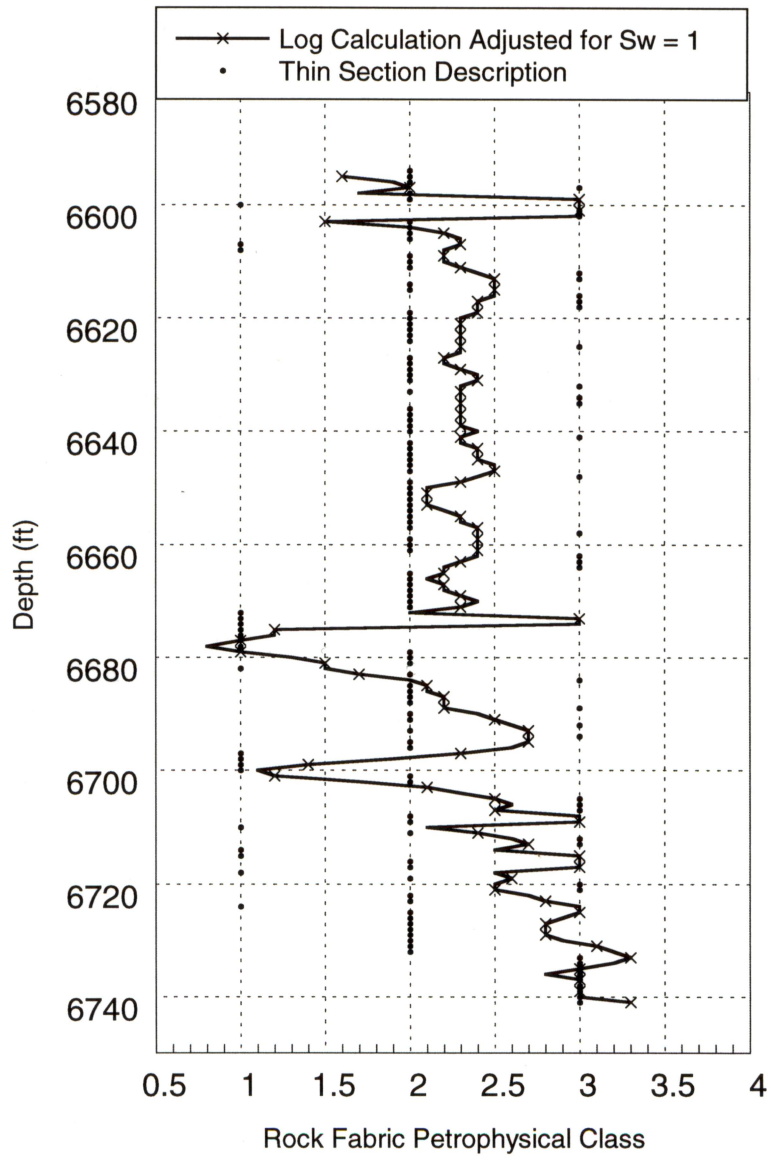


Figure 23. Comparison of petrophysical classes from logs and thin sections for well HRDH 106.

Permeability Calculation from Wireline Logs

Permeability is calculated from wireline logs by substituting petrophysical class and interparticle porosity into the global permeability transform equation. Because of the suspected effect of touching vugs on acoustic-log response in well 101, total porosity was used instead of interparticle porosity from the acoustic log. The rock-fabric term could be eliminated, resulting in a relationship between permeability, saturation, porosity, interparticle porosity, and reservoir height. The link between petrophysical properties and geological parameters, however, is maintained by including the rock-fabric term. This inclusion is important because geological parameters, such as rock fabrics, are required to extrapolate petrophysical properties into 3-D space.

Comparing log-calculated permeability with core permeability shows a good correlation (fig. 24, 25). The high- and low-permeability values are retained in this analysis. Spikes in the core data caused by small-scale heterogeneity are smooth because the logs average over a 2- to 3-ft interval. In well 101, calculated permeability values in interval 6,575 to 6,595 are lower than expected. This interval is interpreted to contain a touching-vug pore system composed of enlarged fractures and small cavities. The rock-fabric petrophysical-class approach does not apply to this pore type. The calculated water saturation is too low, resulting in a petrophysical class that is too low and a calculated permeability that is too low. The rest of the calculated permeability values compare well with core values.

CONCLUSIONS

Analysis of thin sections and core data demonstrates that rock fabrics can be grouped into petrophysical fields defined by porosity and permeability (fig. 26). Grainstones and large crystal dolostones fall within the petrophysical class 1 field of Lucia (1995). Permeability increases with increasing dolomite crystal size. The class 1 field is enlarged slightly to include large crystal dolostones having crystal sizes as much as 300 microns. Grain-dominated and dolomitic mud-

HRDH 101

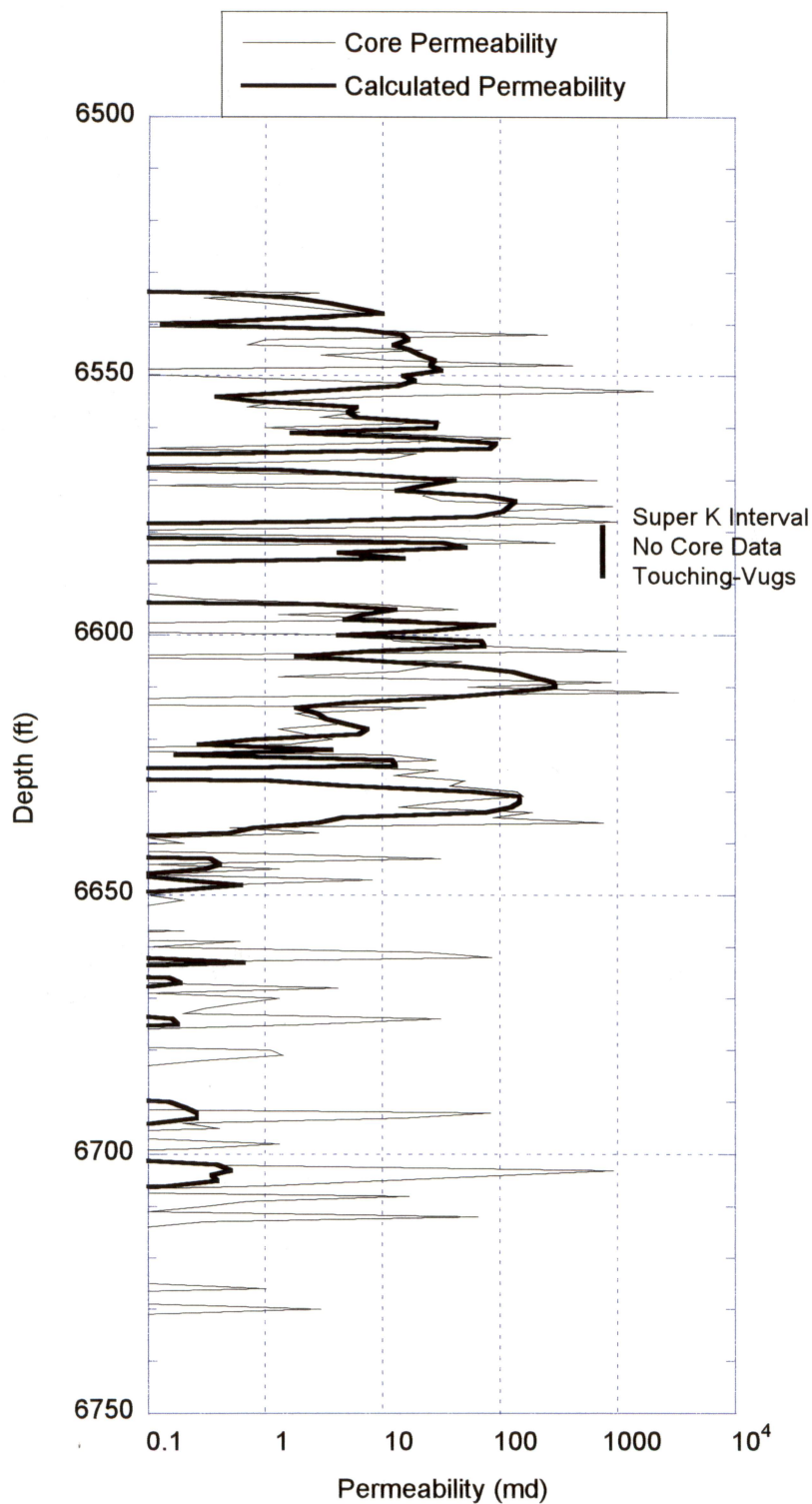


Figure 24. Comparison of core and log-calculated permeability values for well HRDH 101. Permeability values in the super-k interval of HRDH 101 are too low because water saturation and petrophysical class are incorrectly determined.

HRDH 106

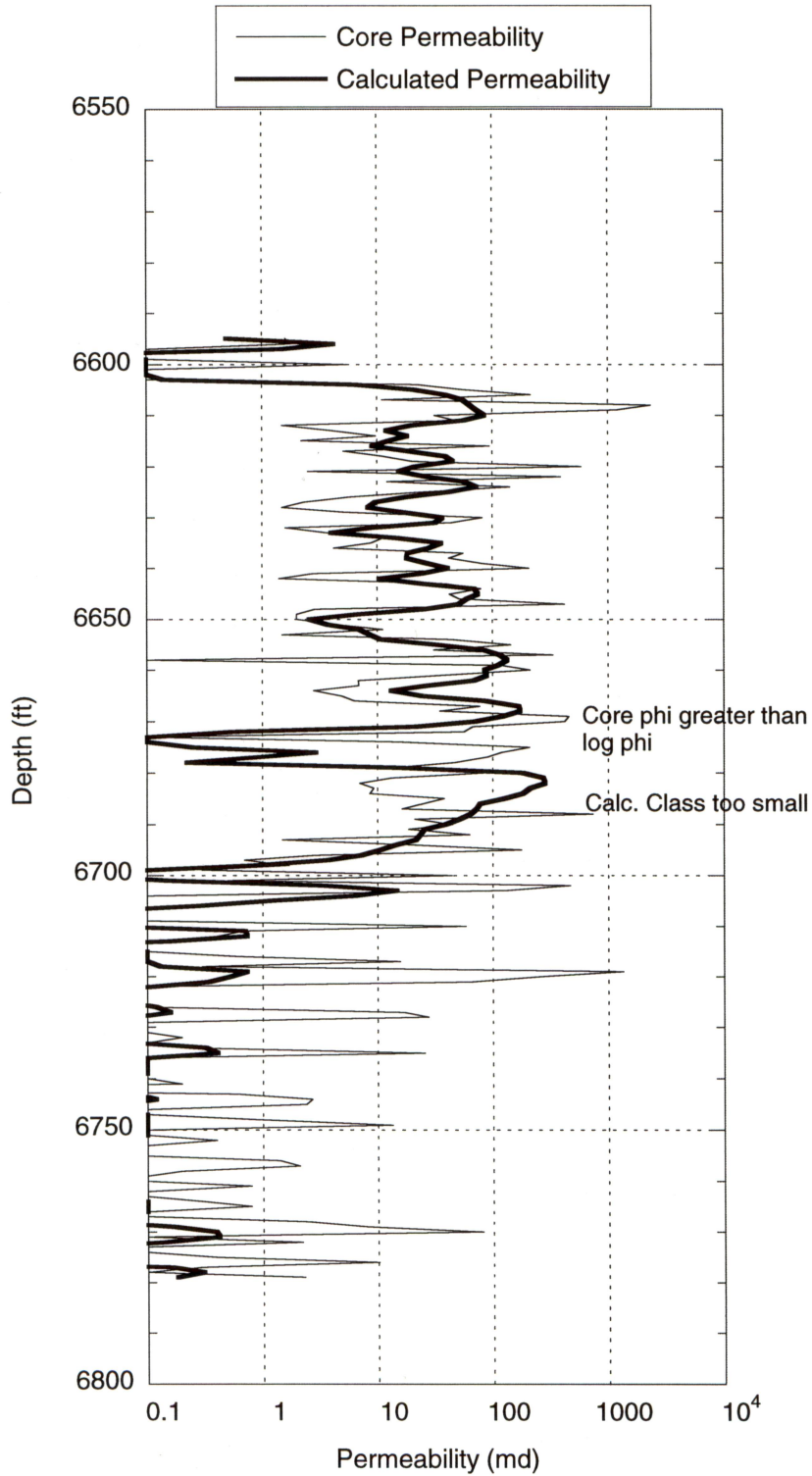


Figure 25. Comparison of core and log-calculated permeability values for well HRDH 106. Permeability in the dolomite interval is too low because log porosity is lower than core porosity.

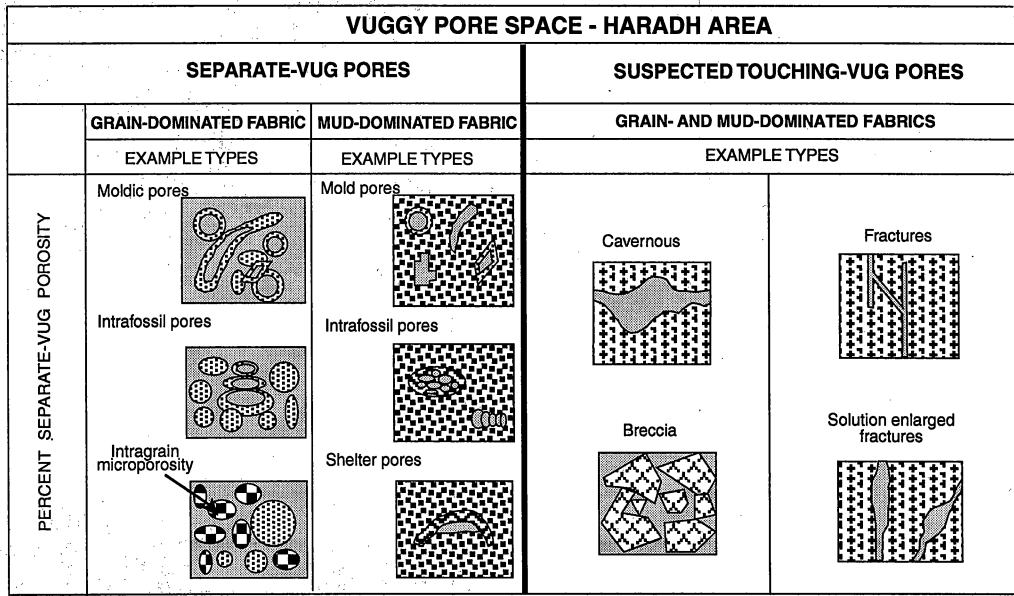
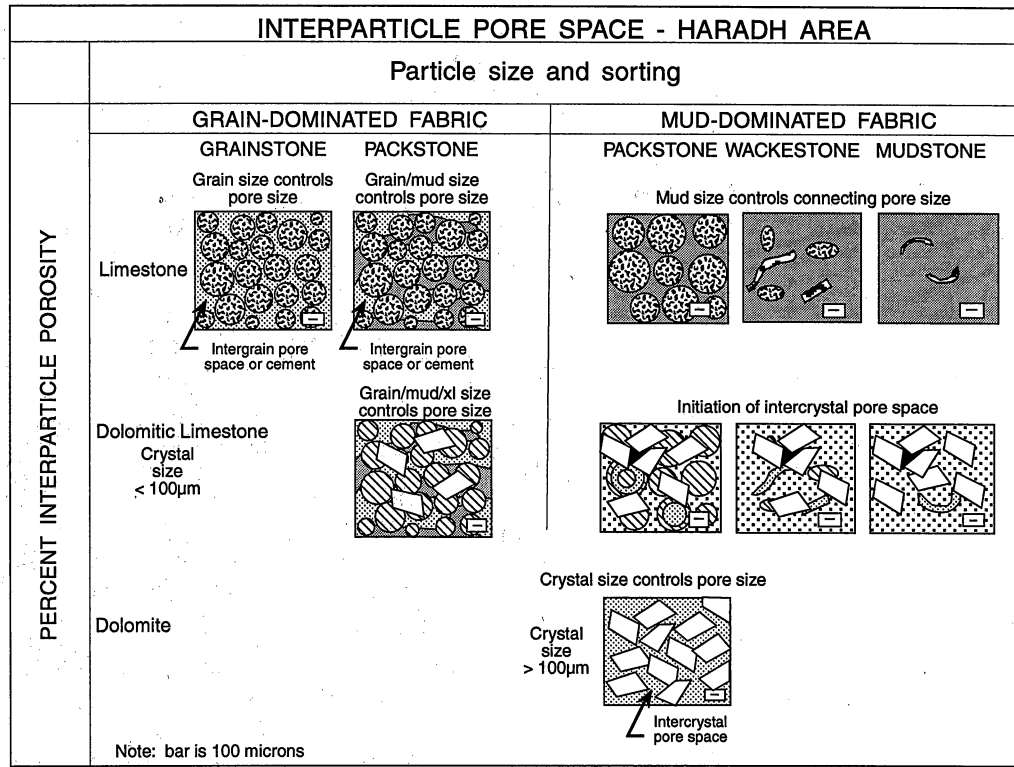


Figure 26. Diagram summarizing rock fabrics found in thin sections of wells HRDH 101 and 106.

dominated fabrics having more than 25 percent dolomite fall into the petrophysical class 2 field. The dolomitic mud-dominated fabrics plot in the class 2 field because progressive dolomitization increases pore size by increasing porosity in the intercrystal mud and by creating intercrystal pore space. Mud-dominated fabrics that have less than 25 percent dolomite are mostly dense, but when they are permeable, plot in the petrophysical class 3 field.

The three generic rock-fabric porosity–permeability transforms developed by Lucia (1995) can be used for this suite of rocks. The permeability of the dolomite, however, may be understated because the class 1 transform does not account for larger than 200-micron crystal size. A global relationship between rock-fabric petrophysical class, interparticle porosity, and permeability that does not require fabrics to be divided into specific petrophysical classes has been developed and is used in this analysis:

$$\text{Log}(k) = (A + B \times \text{Log}(\text{Class})) + (C + D \times \text{Log}(\text{Class})) \times \text{Log}(\Phi_{ip}),$$

where

$$A = 9.7982,$$

$$B = 12.0838,$$

$$C = 8.6711,$$

$$D = 8.2065,$$

and

Class = Rock-fabric petrophysical class ranging from 0.5 to 4

Φ_{ip} = Fractional interparticle porosity

Permeability can be estimated from wireline logs by using the rock-fabric method.

Interparticle porosity is estimated by subtracting total porosity from separate-vug porosity, which, in turn, is estimated from transit-time–porosity cross plots according to the following general equation, which incorporates lithology changes from limestone to dolostone:

$$S_{vug} = (13,406 - D_f \times 8,753) \times e^{-0.32(\Delta t + 141.5 \times \phi)},$$

Petrophysical classes can be identified from a cross plot of water saturation and porosity. The wells are far enough above the free-water level that reservoir height is not an important consideration. Well data from various structural positions and capillary-pressure data should, however, be used in the future to incorporate a reservoir-height term in the equation given next. Boundaries between rock-fabric classes were identified and multiple-regression analysis was used to develop the following relationship between petrophysical class, saturation, and porosity:

$$\text{Log (Class)} = (A + B \log(\phi) + \log(S_w)) / (C + D \log(\phi)),$$

where

Class = Rock-fabric petrophysical class ranging from 0.5 to 4,

$$A = 3.1107,$$

$$B = 1.8834,$$

$$C = 3.0634, \text{ and}$$

$$D = 1.4045.$$

Identifying rock fabrics from log-calculated petrophysical classes requires additional information because (1) there are multiple rock fabrics in each class and (2) the saturation approach applies only to permeable intervals. Class 1 includes both large crystal dolomite and grainstone. Lithology can be used to distinguish between them. Class 2 includes grain-dominated packstones, dolomitic grain-dominated packstones, and dolomitic mud-dominated fabrics. Lithology can be used to distinguish grain-dominated packstones but not to distinguish between dolomitic grain-dominated packstones and dolomitic mud-dominated fabrics. Class 3 includes mud-dominated fabrics that have less than 25 percent dolomite. Because most dense samples are mud-dominated and dolomitic mud-dominated fabrics, low-porosity intervals are assigned to class 3.

Permeability is calculated by substituting log-calculated interparticle porosity and log-calculated petrophysical class into the global transform equation. These calculations compare well with core data and retain high and low permeability values. It is important to retain the rock-fabric petrophysical class term in this calculation because it provides the link between petrophysical properties and geologic processes necessary to display permeability, porosity, and water saturation

in 3-D. Without the tie to stratigraphy, deposition, and diagenesis, log-calculated petrophysical properties cannot be realistically distributed in 3-D space.

The super k interval in well 101 appears to be producing from a touching-vug pore system composed of small caverns and fractures. The extensive amount of large crystalline dolostone around this touching-vug pore system suggests that the touching-vug pore system also provided the flow path for dolomitizing fluids. The large size of the dolomite crystals is consistent with burial or late origin for the dolomite. Assuming the dolomitization is late, the pore space of the precursor limestone may have been similar to the present limestone, and the dolostone may have inherited its porosity values from the precursor limestone. This would explain why the limestone, dolomitic limestone, and dolostone have similar porosity ranges. The important impact of dolomitization is increased pore size in the mud-dominated and grain-dominated packstone fabrics to a size similar to or larger than that of permeable grainstones.

REFERENCES

- Harari, Zake, Sang, Su-Tek, and Saner, S., 1995, Pore-compressibility study of Arabian carbonate reservoir rocks: *Society of Petroleum Engineers Formation Evaluation*, v. 10, n. 4, p. 207–214.
- Lucia, F. J., 1983, Petrophysical parameters estimated from visual description of carbonate rocks: a field classification of carbonate pore space: *Journal of Petroleum Technology*, March, p. 626–637.
- _____, 1995, Rock fabric/petrophysical classification of carbonate pore space for reservoir characterization: *American Association of Petroleum Geologists Bulletin*, v. 79, no. 9, p. 1275–1300.

Powers, R. W., 1962, Arabian Upper Jurassic carbonate reservoir rocks, *in* Ham, W. E., ed., Classification of carbonate rocks, American Association of Petroleum Geologists Memoir 1, p. 122–192.

Wang, R. F. P., and Lucia, F. J., 1993, Comparison of empirical models for calculating the vuggy porosity and cementation exponent of carbonates from log responses: The University of Texas at Austin, Bureau of Economic Geology, Geological Circular 93-4, 27 p.

APPENDIX 1
Petrographic Data for Wells HRDH 101 and 106

Well No.	Plug#	Depth	Dolomite		Calcite		Sulfate		Accessories		Texture		Psv		Core Analysis		Comments						
			%	Size(um)	%		% Anth	Type	%	Type	% Grain	% Mud	Gm Size	% PIP	% Psv Type	% GIU Grams		Class	% Por	% P	% Psv	Perm	
101	360	6723.0	0.6	40	99.4	0.0	0.0	0.0			41.0	59.0	<20	0.0	0.0	IF	0.0	3	7.3	7.3	0.0	0.0	compacted GDP?
101	362	6724.0	1.7	60	98.3	0.0	0.0	0.0			51.8	48.0	300	0.3	2.6	IF	1.0	3	7.7	5.1	0.1	0.1	
101	364	6725.0	13.1	120	86.5	0.0	0.0	0.0			64.9	35.1	300	2.6	1.0	IF, MO	0.0	3	6.7	5.7	0.1	0.1	cladocropis, clasts
101	366	6726.0	100.0	80	0.0	0.0	0.0	0.0			0.0	0.0	0.0	0.0	0.0		0.0	1	1.4	1.4	1.0	1.0	
101	368	6727.0	100.0	110	0.0	0.0	0.0	0.0			0.0	0.0	0.0	1.0	0.0		0.0	1	2.7	2.7	0.0	0.0	strange relict shape
101	370	6728.0	9.1	90	90.4	0.0	0.0	0.0			47.2	52.8	<20	0.3	0.6	IF, MO	0.0	3	4.8	4.2	0.1	0.1	stylolite 0.3 insoluble residue; burrow
101	372	6729.0	5.7	90	93.4	0.0	0.0	0.0			61.8	38.2	250	0.6	0.0	IF, MO	0.0	2	5.5	5.5	0.1	0.1	
101	374	6730.0	0.6	80	99.0	0.0	0.0	0.0			81.3	18.6	300	1.0	2.6	IF, MO	0.6	2	10.8	8.2	2.9	2.9	cladocropis frags
101	376	6731.0	38.7	80	61.3	0.0	0.0	0.0			2.6	97.4	<20	0.0	0.0		0.0	3	1.6	1.6	0.1	0.1	
101	378	6732.0	25.1	80	74.3	0.0	0.0	0.0			18.0	82.0	<20	0.0	0.0		0.0	3	2.4	2.4	0.0	0.0	burrow
101	380	6733.0	7.0	60	93.0	0.0	0.0	0.0			3.9	96.1	<20	0.0	0.0		0.0	3	2.9	2.9	0.1	0.1	
101	382	6734.0	13.6	90	85.7	0.0	0.0	0.0			8.9	91.1	<20	0.0	0.0	MO, IF	0.0	3	4.6	4.6	0.1	0.1	burrow
101	384	6735.0	43.4	60	56.3	0.0	0.0	0.0			26.4	73.6	<20	0.0	0.0		0.0	2	3.0	3.0	0.1	0.1	burrow
101	386	6736.0	55.4	80	44.6	0.0	0.0	0.0			1.3	98.7	<20	0.0	0.0		0.0	2	1.9	1.9	0.1	0.1	burrow